

<https://doi.org/10.1038/s44296-025-00059-7>

# Improving process granularity of life cycle inventories for battery grade nickel

**Sophia Roy<sup>1</sup>, Hossam Moustafa<sup>1</sup>, Ketan Vaidya<sup>2</sup>, Jean-Philippe Harvey<sup>1</sup> & Louis Fradette<sup>1</sup>✉**

Batteries are essential to transition to a fossil-free energy system, but only if coherently planned will their manufacturing generate minimal environmental impacts. Aggregated life cycle inventories for battery-grade nickel prevent life cycle analysts from easily pinpointing key impact contributors. The present work reconstructs inventories via disaggregation of current and emerging processing routes. Improving process granularity demonstrates variability in climate impacts of 74 kgCO<sub>2eq</sub>/kWh for nickel sourcing of an NMC-811 cell. Furthermore, the global ecoinvent v.3.9.1 dataset for nickel sulfate could gravely underestimate climate impacts by 120 kgCO<sub>2eq</sub>/kg Ni equivalent. Major contributors to climate impacts are readily identified for six nickel processing pathways, spanning two mineral families – laterite and sulfide – and three main processing routes – hydrometallurgy, bioleaching and pyrometallurgy. A preliminary assessment of all impact categories highlights the need for both improved fate models and data collection on inventory parts such as tailings management which are often neglected in carbon-focused studies.

Batteries are an essential part of the transition to a fossil free energy system. However, only if coherently planned will the manufacturing of battery cells generate minimal climate change impacts. Large-scale cell production impacts can be broadly divided into two main contributing categories: energy consumed to manufacture the battery cell, and upstream processing pathways embodied in the cell materials<sup>1</sup>. Even if few existing battery LCAs source primary data for cell production<sup>2</sup>, the assessment of a perfectly accurate primary model (i.e. zero uncertainty for energy and materials consumption data) will still exhibit high uncertainty due to its background data. For instance, a recent parametric LCA study found that climate change impacts of raw materials for a nickel-manganese-cobalt (NMC-811) battery cell may quintuple from 23 to 106 kgCO<sub>2eq</sub>/kWh, depending on the production routes which supplied its materials. For lithium-iron-phosphate (LFP), emissions from raw materials could triple from 21 to 58 kgCO<sub>2eq</sub>/kWh<sup>3</sup>.

For the aforementioned analysis, ranges of carbon intensities of each cell material were compared to available life cycle data, wherefrom production routes are often found to be aggregated via weighted averages of regions or markets<sup>3</sup>. Aggregation renders it difficult to discretize the cell's carbon footprint as a function of technology and location specific parameters in materials supply chains<sup>4</sup>. The same conclusion holds true for prospective assessments conducted on aggregated datasets, which do not retain the required granularity to model process-level technological improvements.

On the other hand, parametrization allows to target key improvements in the supply chain of a material which synchronously improves the carbon footprint of the battery cell<sup>5</sup>. A specific and quantified contribution analysis of underlying material extraction and refining processes in the supply chain of each cell material would allow for the ideal level of granularity in order to reduce inherent uncertainty in current battery cell life cycle inventories (LCIs). The present study proposes a deep dive into one of the material pillars of an NMC gigafactory supply chain – nickel - in order to better understand how to conduct such investigation.

Most recent publications in the field of prospective life cycle assessment (PLCA) make use of integrated assessment models (IAMs) for background modelling<sup>6–12</sup>. Since IAMs do not contain detailed scenarios for the evolution of metal markets, future scenarios had to be developed. To generate future scenarios for seven metals (copper, nickel, zinc, lead, iron, aluminum, and manganese), unit processes from the ecoinvent v2.2 database are updated according to predicted energy mix and energy consumption increase from global ore degradation<sup>13</sup>. This work was later extended to generate future scenarios (for copper, nickel, zinc and lead only) which include futurized electricity mix, project improvements in energy efficiency and model market share development (in terms of production locations and primary/secondary share)<sup>10</sup>. While specific process data was collected to model primary production routes of metals, their aggregation into global averages with a fixed ore grade results in granularity losses<sup>13,14</sup>. Considering only one average process model hinders the expression of previously stated high variability in the metal's environmental impacts<sup>3</sup> and the analysis of its

<sup>1</sup>Department of Chemical Engineering, Polytechnique Montreal, Montreal, QC, Canada. <sup>2</sup>Department of Sustainability, Northvolt AB, Stockholm, Sweden.✉e-mail: [louis.fradette@polymtl.ca](mailto:louis.fradette@polymtl.ca)

main contributors. To obtain a global market mix, a ratio of pyrometallurgy to hydrometallurgy production was extrapolated from historical trends, excluding emerging routes under the assumption that they would not own a significant production share before 2050<sup>10,14</sup>.

When conducting prospective background modelling of lithium-ion battery (LIB) industrial ecosystems, the *premise* tool<sup>15</sup> developed for PLCA relies on IAM scenarios to update impact factors of global ecoinvent v.3.8 LIB datasets imported for three NMC variants (NMC-111, -622, -811)<sup>16</sup>, LFP<sup>17</sup> and multiple emerging cathode chemistries. Therefore, when the switch to nickel-rich chemistries<sup>18</sup> or the future carbon footprint of LIB production<sup>7,19</sup> is assessed, only improvements in the electricity and fuels mix are included. The metals comprising the active cathode material are modelled without any changes in their manufacturing methods, and emerging production routes are excluded from the study. This methodological choice also overlooks the fact that not all processing pathways making the historical global metal market meet the purity required for precursors of LIBs. Such lack of technological representativeness in current LCA databases does not provide a strong incentive for cathode active material manufacturers to source raw materials from producers with eco-conscious process alternatives that are more expensive to install and operate. For nickel-rich chemistries specifically, currently expanding supply chains of nickel are not explicitly represented.

The ecoinvent v.3.9.1 database only includes one inventory for nickel sulfate, as a global dataset<sup>20</sup>. Therefore, current LCAs and PLCA mostly rely on the global inventory to model the nickel supply chain of NMC batteries. The ecoinvent dataset for nickel sulfate is constructed to receive nickel class I as a feed from a global market, resulting in a weighted average of nickel sulfate carbon footprints. The distribution of production routes, which are also an aggregation of pyro- and hydrometallurgy routes, includes co-production with cobalt (~50%), smelting and refining of sulfide ores (~30%) and co-production during platinum group metal extraction (~20%). The multiple layers of aggregation in the inventory for nickel sulfate makes it quite challenging to pinpoint key contributors in its supply chain<sup>21</sup>.

Based on recent Monte Carlo simulation results for the global LIB supply chain, it was found that nickel sulfate is the main contributor (~80%) to the expressed variance of climate change impacts for an NMC-811 cell<sup>22</sup>. Such important variation is explained by the delta between carbon footprints of different nickel producers and the nickel-rich nature of the chosen chemistry. One main limitation highlighted in the Monte Carlo simulation study is its reliance on cost data from a commercial provider, with limited data coverage and methodological transparency<sup>22</sup>, in order to perform the disaggregation of carbon footprints. Therefore, the authors pressed the need for an in-depth mapping of the entire supply chain<sup>22</sup>. This echoes previously demanded improvement in the impact factors of material refining processes, which should ideally have disaggregated electricity impacts and be distinguished by suppliers (e.g. industrial plant, supply regions, ore types, etc.)<sup>8</sup>.

While a regional mapping of nickel has been previously performed; Indonesia, which is exponentially increasing its capacity as first global producer<sup>23</sup>, was not part of the studied geographies<sup>24</sup>. Furthermore, regionalized inventories were created by only adjusting the electricity profile and SO<sub>2</sub> emission rate of a high-level global dataset for nickel class I refining. A thorough review of existing PLCA studies on metals revealed that twice as many studies change background electricity mix compared to technology switch in the mineral processing route<sup>25</sup>. For nickel specifically, no studies investigated technology switch, which is again surprising since battery grade nickel feedstocks are currently multiplying.

Traditionally, class I nickel, produced primarily for stainless steel manufacturing, was the only metal powder feedstock compatible with battery purity (99.8%) specifications<sup>26</sup>. Use of class I nickel requires an additional step of chemical dissolution into nickel sulfate before being used for the cathode active material production<sup>1</sup>. On the other hand, mixed hydroxide precipitate (MHP) which contains nickel under hydroxide form but also cobalt and manganese traces, is an emerging feedstock compatible with NMC chemistry. While 300,000 tonnes of nickel class I were produced

in 2021<sup>27</sup>, it is predicted that ~800,000 tonnes of nickel in MHP will be available in 2025 from Indonesia alone<sup>28</sup>. MHP is obtained through high-pressure acid leaching (HPAL) of laterite ores<sup>29</sup> but can also be obtained through bioleaching processing of low-grade nickel deposits<sup>30</sup>. Mixed sulfide precipitate (MSP), containing nickel and cobalt under sulfide form, is another type of intermediate product from bioleaching operations<sup>30</sup>.

Emerging secondary processing routes include hydrometallurgical recycling of spent lithium-ion batteries yielding nickel sulfate<sup>31</sup> or NMC precursor<sup>32</sup> which can directly re-enter the life cycle of new batteries. In addition, re-processing of nickel-bearing tailings is being considered through energy efficient routes such as tank and heap bioleaching<sup>30,33</sup>. One could also envision spent consumer electronics (also commonly referred to as e-waste) to supply second life nickel. While some nickel is currently recovered from e-waste via smelters, novel hydrometallurgical recycling and purification pathways sourcing are under development in order to meet battery specifications<sup>34</sup>.

The multiplication of feedstocks implies that future nickel stocks will not come from the existing market mix of primary routes as currently modelled in IAMs prospective scenarios. A recent review of nickel sulfate life cycle inventories pressed the need for technology specific and ore grade specific primary data, which is representative of future nickel sulfate production<sup>4</sup>. There is an opportunity to evaluate technological switches now, in order to guide the design of nickel supply chains which will expand in the coming years.

Nickel originates from two main families of ore bodies — sulfide and laterite ores, the latter mainly found in tropical forest regions<sup>28</sup>. While the production of nickel sulfate was historically dominated by high-grade sulfide ore deposits, it is predicted that laterite ore processing will take over the near-term market<sup>22</sup>. Sulfide ore deposits are most commonly found underground, and the ore often requires beneficiation (communition, flotation) before being further processed into refined nickel. Laterite ores, which can contain both nickel-bearing limonite and saprolite minerals, are extracted during open-pit operations, where moisture-rich ores require fewer concentration steps (sieving and dissolution). Limonite is often preferred for HPAL, due to the lower content of magnesium oxide<sup>35</sup>. Saprolite is typically processed in a rotary kiln and electric furnace to produce nickel pig iron (NPI, class II nickel), which can be further refined into battery-grade nickel sulfate when entering a circuit of leaching, solvent extraction and evaporative crystallization steps<sup>36</sup>. Other less widespread processing pathways include atmospheric tank and heap leaching, the Caron Process, the direct nickel process and enhanced pressure acid leaching (EPAL), which combines HPAL of limonite and atmospheric leaching of saprolite sections<sup>37,38</sup>. Each process is adapted to specific impurities (e.g. magnesium and silica) and ore grades of the mineral sections<sup>38</sup>.

Ore grade impacts the quantity of rock that needs to be mined in order to achieve a certain production level. Since mining inventories differ for laterite and sulfide ores, ore grade decline will have different environmental implications for both. Energy consumption correlations as a function of ore grade are currently provided in the literature on a global scale for both sulfide and laterite ores<sup>14</sup>. However, material inventories are assumed constant due to data unavailability<sup>39</sup>. In practice, the deposit's stripping ratio, which describes the amount of waste rock that needs to be removed in order to access the ore, will also affect the material inventory (e.g. explosives and backfill binder requirements)<sup>40</sup>. Therefore, remodelling mining and beneficiation inventories as a function of site-level ore grade and stripping ratio would allow to account for the variability between sites. Since primary inventories of nickel mining operations are scarce, the quantity of rock mined becomes relevant to scale available inventories.

Process-based LCIs can provide the mass and energy balances required to generate technology specific inventories when primary data is unavailable<sup>41</sup>. Greenhouse gas, energy and water assessments for HPAL and rotary-kiln-electric-furnace (RKEF) processing of laterite ores, with subsequent conversion routes into nickel sulfate were previously obtained by directly extracting mass and energy balances from Aspen Plus flowsheets<sup>36</sup>. A process-level LCA of nickel sulfate production compared the carbon

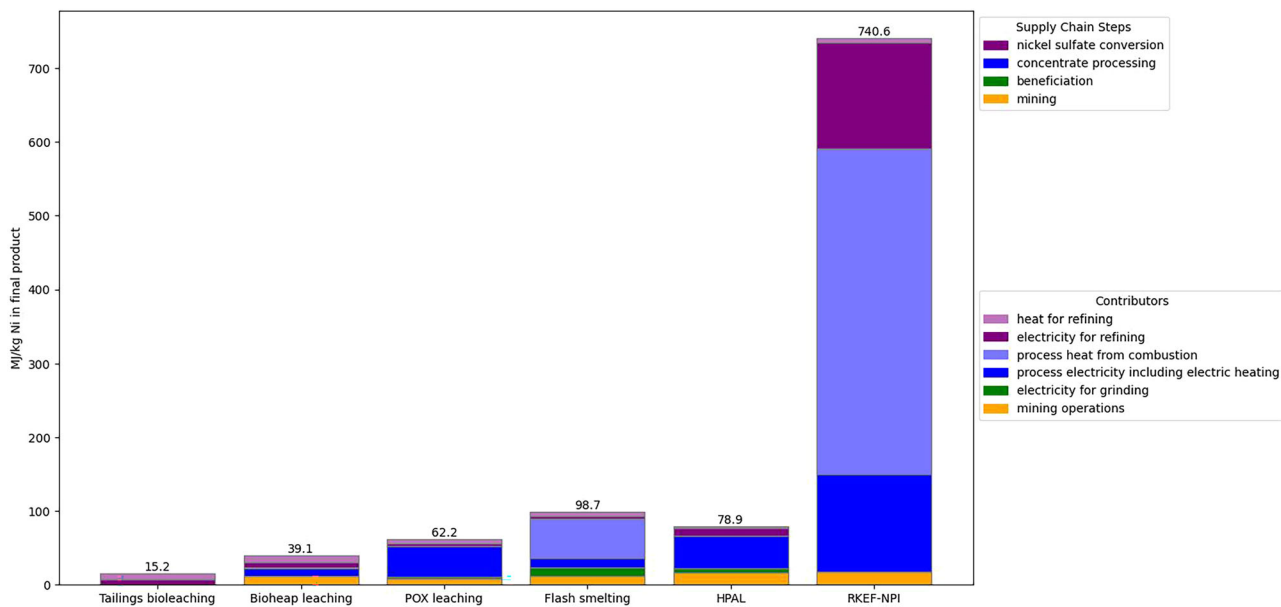


**Fig. 1 | Absolute comparison of the direct energy demand of modelled nickel processing routes.** Contributors are associated via color tone to one of the four supply chain steps — orange for mining, green for beneficiation, blue for concentrate processing and purple for nickel sulfate conversion— and are cumulated to the overall direct energy requirements. From left to right, four sulfide concentrate processing, and two laterite pathways are ranked from lowest to highest energy requirements in their own sub-type of ore processed. Emerging bioleaching alternatives, namely tailings bioleaching and bioheap leaching exhibit the lowest energy requirements to reach battery-grade nickel sulfate. Hydrometallurgical processes offer lower direct energetic consumptions to process nickel ores to battery-grade nickel sulfate than

pyrometallurgical processes. For pyrometallurgical pathways, it is important to note that process assumptions regarding the operating temperature as well as the incoming ore grade or nickel content of the concentrate will highly influence the resulting heat requirements of modelled kilns and furnaces. For flash smelting, the dried concentrate (11.5%) is charged at 25 °C, while the flash furnace temperature is assumed to reach 1450 °C via combustion of diesel and coal<sup>42</sup>. For the RKEF-NPI pathway, the underlying process simulation assumes that the incoming ore (1.22% Ni) is dried using hot gas from the rotary kiln, supplemented by the combustion of natural gas, before being mixed with coal and heated to 800°C in the rotary kiln<sup>36</sup>.

footprint of the HPAL and RKEF-NPI routes for laterite ore processing with the flash smelting of sulfide ore<sup>35</sup>. Process-specific disaggregation was pushed one step further down the value chain by building process models for mining and beneficiation steps of sulfide and laterite ores.

Often times, process-specific inventories are only available for the concentrate processing steps. For instance, a methodology was also published to derive mass and energy balances for flash smelting of sulfide ores, as well as RKEF and blast furnace pyrometallurgical treatments of laterite ores, in order to calculate the embodied energy and carbon footprint, but cannot readily provide information about further refining into nickel sulfate<sup>42</sup>. Furthermore, such inventories are designed specifically for carbon footprint assessment and neglect contributors to other impact categories such as tailings and emissions to air and water. A high-level life cycle inventory of HPAL is available but does not provide a process model for tailings management<sup>43</sup>. In extreme cases, inventories for HPAL and RKEF neglected the mining and beneficiation part of the value chain<sup>44</sup>. Since the aforementioned study only considered the carbon footprint indicator, deep-sea mining of polymetallic nodules was also presented as a promising low-carbon route, without assessing critical risks on the deep sea marine environment.

To the best of the authors' knowledge, no complete process-based LCIs are currently available in the ecoinvent v.3.9.1 database for the bioleaching of sulfidic concentrate and tailings, for pressure oxidation leaching (POX) of sulfide ores, for nickel pig iron conversion and for the high-pressure acid leaching of nickel laterite ores. Furthermore, no comparative LCA study presents disaggregated technology specific inventories for battery-grade nickel production, from mining to refining, based on different energy mix, ore grade, strip ratio and reagents consumptions considered.

The desired outcome of the present study is to develop a process-based method to generate background life cycle inventories for current and prospective studies with increased granularity in terms of technological representativeness. To better illustrate the potential findings from our

developed method, we apply it to the nickel sulfate supply chain for lithium-ion battery manufacturing. The resultant is a variety of potential carbon footprints, embodied energies and midpoint environmental impacts for nickel sulfate, instead of a conventional fixed value. From that starting point, prospective improvements can be identified for major contributing parameters throughout the supply chain.

## Results

### Direct embodied energy of modelled pathways

As a first comparison point, Fig. 1 presents the direct embodied energy (or primary energy demand) of modelled nickel processing pathways. Transport energy requirements are removed from the assessment, since they are not process-specific and will vary depending on the locations of mining, processing and refining facilities. The RKEF-NPI route is ~9× more energy intensive than its laterite hydrometallurgy processing counterpart, and ~50× more than sulfidic tailings bioleaching. Direct embodied energy is a key contributor to the potential climate impacts of concentrate processing pathways, especially with fossil fuel intensive energy mixes. Compared to pressure oxidation leaching, bioleaching alternatives are attractive for nickel sulfide processing in regions where industrial blocks of renewable electrical power are scarce. Pyrometallurgical processing pathways exhibit a higher share of thermal energy to electricity, which may be less straightforward to decarbonize (refer to the light blue versus dark blue shades of the flash smelting and RKEF-NPI bars).

For comparison, while we obtain 98.7 MJ/kg Ni<sub>eq</sub> for the flash smelting route, energy requirements for the process system of nickel sulfate in ecoinvent — sourcing nickel class I from the smelting and refining of sulfide concentrate (16% Ni) — sum up to a close value of 94.8 MJ/kg Ni<sub>eq</sub>. When accounting for the materials embodied energy, considering a nickel ore grade of 2.30% instead of the present study's 2.05% (which has an effect to decrease mining and beneficiation energy requirements), and excluding the nickel sulfate conversion step, a previous study obtained a value of 114 MJ/

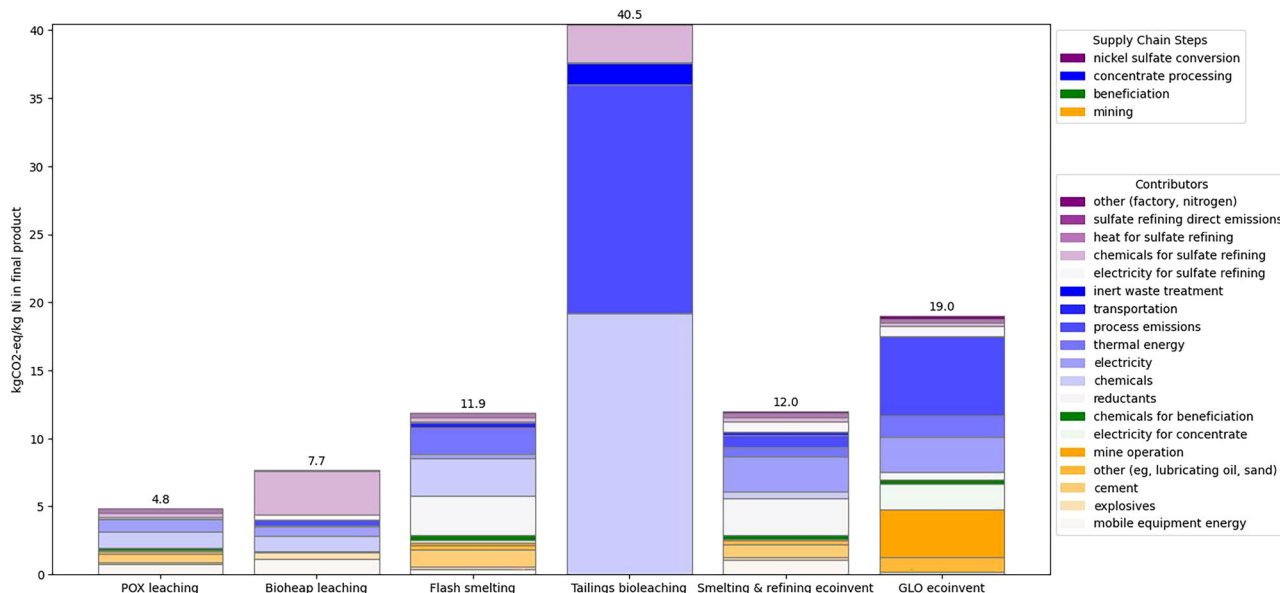


**Fig. 2 | Calculated contributors to climate change impacts of nickel sulfide ore processing routes.** Contributors are associated via color tone to one of the four supply chain steps and are cumulated to the overall climate impacts. The four modelled sulfide concentrate processing pathways are ranked from lowest (POX leaching at 4.8  $\text{kgCO}_2\text{-eq}/\text{kg Ni}_{\text{eq}}$ ) to highest (tailings bioleaching at 40.5  $\text{kgCO}_2\text{-eq}/\text{kg Ni}_{\text{eq}}$ )

$\text{Ni}_{\text{eq}}$ ) cumulative climate impacts per kg of nickel in nickel sulfate hexahydrate, battery-grade. Included for comparison are the resulting climate impacts from the available product system in the ecoinvent v.3.9.1 database for nickel sulfate, via sourcing of nickel class I from smelting and refining of nickel sulfide concentrate (12.0  $\text{kgCO}_2\text{-eq}/\text{kg Ni}_{\text{eq}}$ ), and from the global (GLO) market (19.0  $\text{kgCO}_2\text{-eq}/\text{kg Ni}_{\text{eq}}$ ).

kg Ni in nickel metal<sup>45</sup>, while here we report a value of 89 MJ/kg Ni in nickel metal. The reported difference is most likely due to the exclusion of material embodied energy, reported to make up for ~25% of overall energy requirements in the reference study for the concentrate processing inventory<sup>42</sup>. Removing 25% of the compared embodied energy indeed lands at 86 MJ/kg Ni.

Comparing our reported value of 591 MJ for the RKEF process (without NPI conversion) to a previous study, it is found that 460 MJ are required per kg contained nickel in ferronickel (35% Ni) via RKEF in a coal-based electricity mix or 598 MJ per kg contained nickel in NPI (10% Ni) via the blast furnace route<sup>42</sup>. Ore grades considered in the comparative study are higher than the 1.22% value assumed in our modelling, respectively at 2.20% and 1.88%. However, a lower sensibility to nickel ore grade was found for the overall process energy requirements of laterite-based process than for sulfide-based routes, due to the higher relative contribution of mining and beneficiation for the latter<sup>42</sup>. There exists a broad range of reported energy requirements for NPI production in the literature, depending on the nickel content of the input ore (0.5% to 2.5%) and output alloy (1.5 to 17% Ni), for an average 63 MJ/kg NPI<sup>46</sup>. Considering an NPI quality of 2.9% in our modelling, we obtain a lower estimate of 17 MJ/kg NPI.

### Contributors to climate change impacts of sulfide pathways

It is found that all nickel sulfide ore processing pathways modeled in this work except tailings bioleaching exhibit lower climate change impacts than the ecoinvent dataset, the latter offering values of 12.0  $\text{kgCO}_2\text{-eq}/\text{kg Ni}_{\text{eq}}$  for the smelting route and 19.0 for the global market (GLO) (refer to Fig. 2). This discrepancy can be explained by the majority of these pathways representing hydrometallurgy and bioheap leaching flowsheets, which exhibit lower emissions for concentrate processing (dark blue sections). Indeed, the production routes considered in the ecoinvent dataset first come from the global cobalt production dataset (i.e. mix of roasting, smelting and acid leaching routes), with nickel class I as a co-product<sup>20</sup>. Furthermore, all nickel sulfide pathways present lower mining and beneficiation requirements (orange and green supply chain steps). In a prospective study, this difference would cause the global ecoinvent dataset to falsely overestimate the decarbonization potential of renewable energy for mining and beneficiation operations of sulfide ores (from 6% contribution for flash smelting to 17.5% contribution for

POX leaching, versus 10% for the smelting and refining ecoinvent dataset and 28% contribution for the global ecoinvent dataset). While both smelting inventories exhibit near identical climate impacts, key differences are the contributions of chemicals (23.6% vs 3.9%) and electricity (2.2% vs 21.3%) for nickel class I processing due to the flash smelting pathway modelling ammoniacal precipitation with hydrogen as a refining route, instead of an aggregated mix of electrochemical refining techniques. This distinction exhibits how granularity at the level of nickel class I refining is essential for the definition of detailed decarbonization pathways for nickel.

The embodiment of chemicals is the key contributing factor to climate change impacts of hydrometallurgy and bioleaching routes, both in the concentrate processing and sulfate refining stages (light blue and purple shades in Fig. 2). While bioheap leaching of sulfide ores reduces energy consumption by 60% compared to flash smelting, climate impacts are only reduced by 35% due to high chemical consumption from the lower nickel grade of processed ores. Indeed, to produce 1 tonne of nickel, 587 tonnes of sulfide ores (0.27% Ni) are treated via bioheap leaching, compared to 55 tonnes of sulfide ores (2.05% Ni) for the flash smelting pathway. Similarly, when examining the results for tailings bioleaching, it is found that even if the mining stage is avoided, the extensive use of chemicals for concentrate processing, including limestone and its associated high share of process emissions, makes it more carbon intensive than flash smelting. However, from a mineral resource use perspective, it is expected to perform better, which reinforces the importance of examining environmental performance over multiple impact categories.

### Contributors to climate change impacts of laterite pathways

Regarding laterite ore processing, the RKEF-NPI route may be ~7 times more carbon intensive than the global average reported in ecoinvent (refer to Fig. 3a). Indonesia holds the monopoly on battery-grade nickel sulfate production, currently relying on NPI conversion and investing in new HPAL operations for upcoming expansion<sup>28</sup>. Therefore, RKEF-NPI is the main processing pathway globally, representing nearly 50% of the 2025 Indonesian market, with HPAL at 35% but expected to take over in upcoming years<sup>28</sup>. Looking at the carbon footprint of RKEF-NPI, the GLO ecoinvent dataset significantly underestimates climate change impacts from current nickel sulfate production. The use of coal char as reductant, as well as

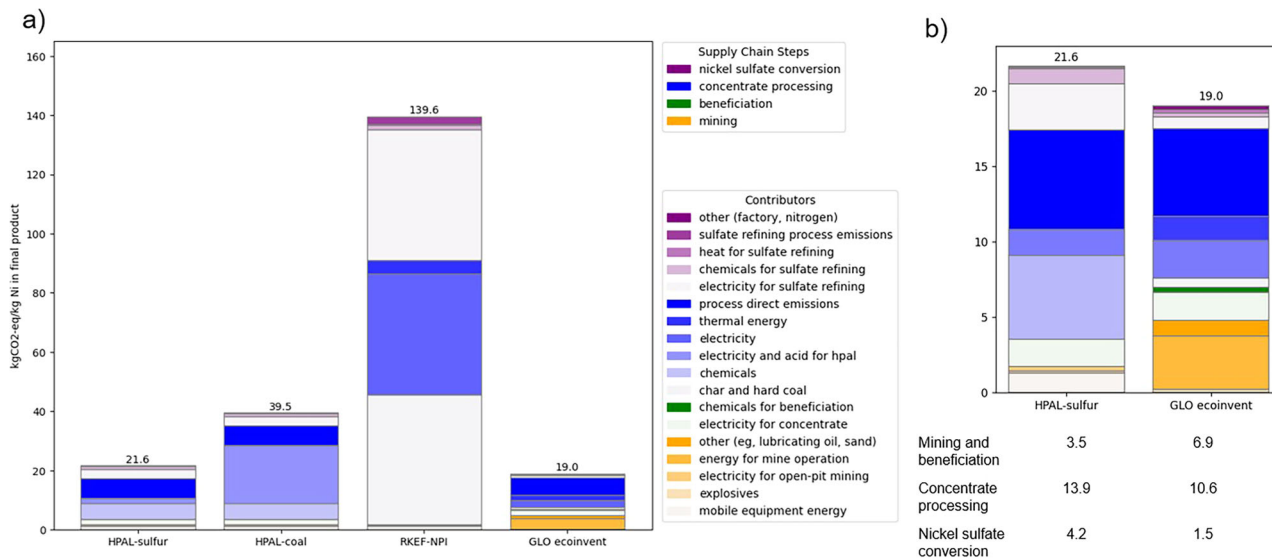


**Fig. 3 | Calculated contributors to climate change impacts of nickel laterite ore processing routes.** Contributors are associated via color tone to one of the four supply chain steps and are cumulated to the overall climate impacts. **a** The HPAL processing route is assessed under two existing process configurations for sulfuric acid production and energy sourcing — on-site sulfur burning (21.6 kgCO<sub>2eq</sub>/kg Ni<sub>eq</sub>) and externally sourced coal(lignite)-based energy and sulfuric acid (39.5 kgCO<sub>2eq</sub>/kg Ni<sub>eq</sub>). The hydrometallurgical pathway is then compared to a pyrometallurgical alternative for laterite ore processing, RKEF-NPI, with climate

impacts summing up to 139.6 kgCO<sub>2eq</sub>/kg Ni in nickel sulfate hexahydrate, battery-grade. **b** Since the sulfur-burning alternative for the HPAL process exhibits similar climate impacts to the global product system for nickel sulfate in the ecoinvent database, a closer comparison is presented on this side of the figure. It is found that the global ecoinvent dataset for nickel sulfate considers a higher contribution of the mining and beneficiation stages, but a lower contribution of concentrate processing and nickel sulfate conversion steps than the HPAL variant.

lignite-based electricity for the arc furnace, and natural gas for thermal energy are causing higher concentrate processing emissions for the RKEF-NPI route (faint to dark blue contributors, representing 64% of the overall footprint). In addition, the lignite-based electricity mix in Indonesia for sulfate refining considerably increases the resulting climate change impacts (contributing to 32% of the overall footprint). Similarly, for HPAL, the distinction is clear (refer to electricity and acid for HPAL contributor in Fig. 3a), with a delta of 17 kgCO<sub>2eq</sub>/kg Ni<sub>eq</sub>) between the configuration which recovers heat from sulfur burning and the configuration which sources electricity from the Indonesian grid mix. It is found that lignite-based electricity consumption contributes to 42% and 61% of climate impacts for the HPAL-coal and RKEF-NPI datasets respectively.

Conducting a prospective assessment of nickel sulfate using the HPAL-sulfur and GLO ecoinvent datasets would yield different conclusions, even if their current climate change impacts are in a similar magnitude (refer to Fig. 3b). For instance, assuming as prospective improvement the renewable electrification of nickel mines, the GLO dataset would exhibit a decrease of ~5.4 kgCO<sub>2eq</sub>/kg Ni in nickel sulfate, while only a saving of 1.3 is found for HPAL. Furthermore, the global dataset's underrepresentation of the contribution of electricity for sulfate refining and of embodied emissions for chemicals would not lead to target these items for decarbonization. On the topic of chemicals, for HPAL, direct CO<sub>2</sub> emissions stem from the use of limestone as a precipitation agent, mainly to remove the iron and aluminum content in nickel-bearing laterite ores. As prospective improvement, switching from limestone to lime would have a high reduction potential for direct CO<sub>2</sub> emissions (~6.6 kgCO<sub>2eq</sub>/kg Ni<sub>eq</sub>) but would increase embodied emissions of the precipitation chemical (0.01 kgCO<sub>2eq</sub>/kg of limestone versus 0.07 kgCO<sub>2eq</sub>/kg lime<sup>20</sup>). In contrast, the main contributor to embodied emissions of chemicals for HPAL is magnesia, with 5.2 kgCO<sub>2eq</sub>/kg Ni<sub>eq</sub> for which low-carbon manufacturing methods are in development.<sup>47</sup>

To assess how Indonesia's reliance on coal electricity affect the climate change impacts of its nickel, we have conducted a scenario analysis in which all electricity inputs are switched to solar electricity (found in Supplementary Tables 10 and 25). For HPAL, the correspond climate impacts reduce to

16.7 (~23%) and 21.4 (~46%) kgCO<sub>2eq</sub>/kg Ni<sub>eq</sub> for sulfur- and coal-powered flowsheets respectively, with a residual contribution for electricity of 1.5% and 3.1%. For the sulfur-powered configuration, direct CO<sub>2</sub> emissions from limestone usage remain the largest contributor to overall impacts (from 31% now 40%) followed by embodied emissions of magnesia (from 24% now 31%). For the previously coal-powered flowsheet, embodied emissions of purchased sulfuric acid also remain a large contributor (from 15% now 28%). For RKEF-NPI, a staggering decrease of climate impacts is observed (~59%) to 57.8 kgCO<sub>2eq</sub>/kg Ni<sub>eq</sub>, with a residual contribution of 6% for electricity. Char and hard coal for calcination now contributes to 76% of climate impacts (previously 31%), followed by natural gas for the drier (8%, previously 3%).

In addition, a scenario analysis on the inevitable ore grade decline of laterite ores from extensive mining was performed (refer to Supplementary Tables 11 and 26). Ore grade is depreciated from 1.22% to a minimum value of 0.5%, consistent to previous sensitivity analyses of ore grade decline on the mining and beneficiation inventories of laterite processing pathways<sup>38</sup>. For HPAL, the resulting contribution of mining and beneficiation stages to climate impacts doubles from 16% to 32%, and from 9% to 19% for sulfur- and coal-powered configurations respectively. Overall climate impacts increase to 26.7 and 44.6 kgCO<sub>2eq</sub>/kg Ni<sub>eq</sub> respectively at an ore grade of 0.5%. For RKEF-NPI, the contribution of the mining stage increases but remains minimal from 1.3% to 3.1%, for a carbon footprint of 142.2 kgCO<sub>2eq</sub>/kg Ni<sub>eq</sub> at an ore grade of 0.5%. To note that impacts on the drying stage are assumed unchanged<sup>38</sup> but could potentially increase.

#### Variation in climate change impacts from a battery cell perspective

From a battery cell perspective, there is an absolute difference of 74 kgCO<sub>2eq</sub>/kWh when assessing climate change impacts of an NMC-811 cell containing 100% nickel sulfate sourced from POX leaching versus from nickel pig iron conversion. If we transpose this delta on an equivalent distance required to compensate for the nickel content of the battery, it results in a difference of ~18,000 km in a hydro-based grid (650 km for POX leaching and 18,700 km for RKEF-NPI).

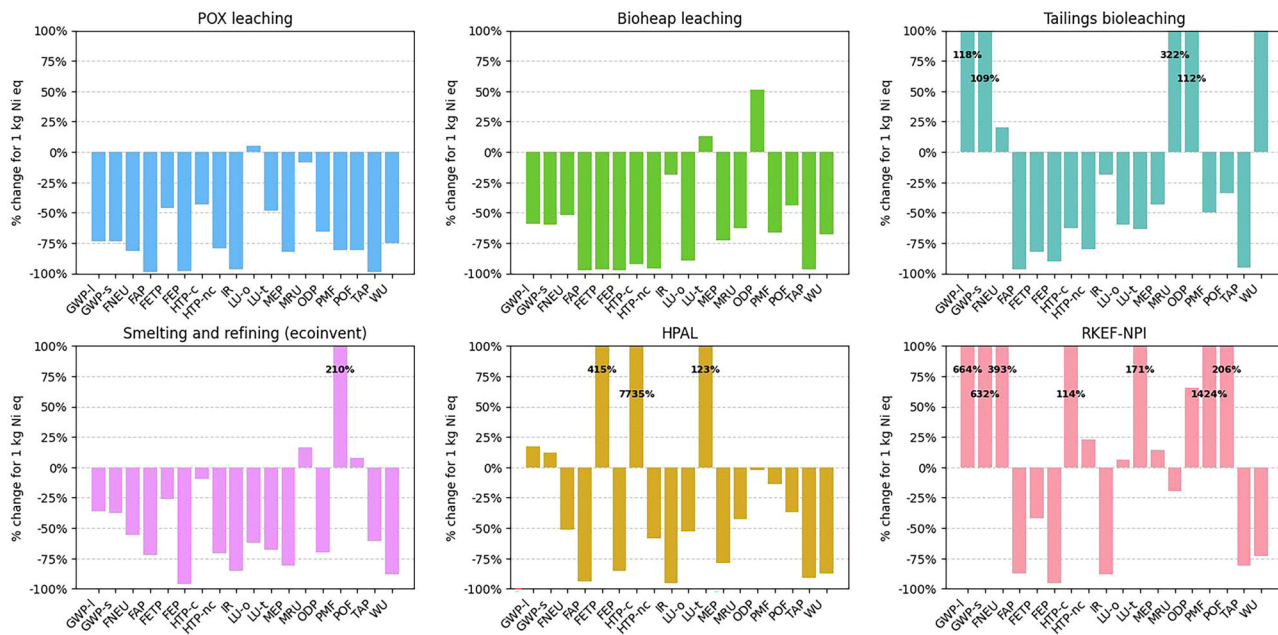


**Fig. 4 | Normalization of midpoint results, via the IMPACT WORLD+ v.1.29 method, as percentage change from the value obtained with the global nickel sulfate dataset in ecoinvent, for 1 kg Ni<sub>eq</sub>.** The six modelled concentrate processing routes are assessed over all midpoint categories to explore any burden shifting risks from prioritizing sourcing via one pathway versus another and to identify life cycle assessment implications of using one particular dataset versus the existing global ecoinvent dataset. To note here that the smelting and refining dataset for nickel sulfide concentrate in ecoinvent was selected in lieu of the flash smelting dataset, due to its better coverage of emissions to air and water. For midpoint results with percentages of change exceeding 100%, the corresponding value is noted directly on the associated bar. Abbreviations: GWP-I: Climate change, long term (kgCO<sub>2</sub>eq),

GWP-s: Climate change, short term (kgCO<sub>2</sub>eq), FNEU: Fossil and nuclear energy use (MJ deprived), FAP: Freshwater acidification (kgSO<sub>4</sub>eq), FETP: Freshwater ecotoxicity (CTUe), FEP: Freshwater eutrophication (kgPO<sub>4</sub>, P-lim<sub>eq</sub>), HTP-C: Human toxicity cancer (CTUh), HTP-nc: Human toxicity non cancer (CTUh), IR: Ionizing radiations (Bq C-14<sub>eq</sub>), LU-o: Land occupation, biodiversity (m<sup>2</sup> arable land eq .yr), LU-t: Land transformation, biodiversity (m<sup>2</sup> arable land<sub>eq</sub>), MEP: Marine eutrophication (kg N, N-lim<sub>eq</sub>), MRU: Mineral resources use (kg deprived), ODP: Ozone Layer Depletion (kg CFC-11<sub>eq</sub>), PMF: Particulate matter formation (kg PM2.5<sub>eq</sub>), POF: Photochemical oxidant formation (kg NMVOC<sub>eq</sub>), TAP: Terrestrial acidification (kg SO<sub>2</sub>eq), WU: Water scarcity (m<sup>3</sup> world<sub>eq</sub>).

The same parallel can be drawn for the embodiment of energy in the nickel content of the battery. Here, only direct energy consumption of the whole nickel processing value chain is considered (that is, neglecting embodied energy in material consumables not involved in combustion). The resulting distances are significantly higher than for embodied carbon dioxide, respectively 8.5 times and 3.5 times for POX leaching and RKEF-NPI. All driving distances are below the range of 200,000 km<sup>48</sup>, which signifies that they can be compensated for over the average use phase of an electric vehicle battery pack. The equivalent distances range from 1300 km for tailings bioleaching to 65,000 km for RKEF-NPI. The direct embodied energy of RKEF-NPI nickel corresponds to around 1/3 of the energy required to transport oneself over the average lifetime of an EV battery pack. In other words, it requires around 5 years of transportation (12,000 km/year<sup>48</sup>) to compensate for the energy required to produce the nickel content of the battery.

### Potential burden shifting risks

The six processing pathways are assessed across all 18 impact categories of the IMPACT WORLD+ v.1.29 method as exhibited in Fig. 4. The corresponding figures generated with the version 2.01 of IMPACT WORLD+ and the ReCiPe 2016 impact assessment method are also available as Supplementary Figs. 1 and 2. Results were normalized as a percentage of change from the value obtained with ecoinvent's global nickel sulfate dataset, on the basis of 1 kg Ni<sub>eq</sub>. This normalization was performed to explore any potential burden shifting risks from 1) prioritizing sourcing from one pathway versus another and 2) using one particular dataset versus the existing global ecoinvent dataset.

It is found that the RKEF-NPI route represents the highest risks of burden shifting towards particulate matter formation (1424%), global warming potential (~650%), fossil and nuclear use (393%), photochemical

oxidant formation (206%) and land transformation (171%). The ecoinvent dataset for smelting and refining of sulfide ores also exhibits a high risk towards particulate matter formation (210%), which is expected due to the pyrometallurgical nature of the process.

Furthermore, the HPAL route presents the highest risk of burden shift towards carcinogenic human toxicity (7,735%) and freshwater ecotoxicity (415%). This conclusion is supported by previous research on the toxic components of HPAL residues<sup>49</sup>. Both impacts increase much further when using the ReCiPe method, to 28,756% and 593% respectively. However, when changing to the v.2.0.1 version of the IMPACT WORLD+ method, both impacts decrease significantly and even become negative (to -41% and -63% respectively). This staggering change is due to a switch in underlying assumption when modelling the fate of metal emissions to groundwater. In the 1.29 version of IMPACT WORLD+, the surface water characterization factor (CF) is used as a proxy for the groundwater compartment, while in the 2.01 version all groundwater CFs are forced to zero<sup>50</sup>. Since the robustness of the indicator is still to be improved, we suggest not to focus on the value of the impact but to keep in mind that metal emissions to groundwater from HPAL tailings management are a key area of concern and uncertainty in terms of human and ecotoxicity.

Bioheap leaching of sulfide ores does not present significant risks of burden shift compared to conventional methods, even considering its air emissions of ammonium sulfate, nickel refinery dust and non-methane volatile organic compounds (NMVOC), as well as emissions to surface water of copper ion, manganese, nickel, sodium, sulfate and zinc. The observed increase of 50% for the ozone depletion category is caused by the release of tetrachloromethane (R-10) to air during chlor-alkali electrolysis via membrane cell. As part of the upstream supply chain, the chlor-alkali process produces the required sodium hydroxide for both nickel sulfide and sulfate refining steps of the bioheap leaching pathway.

Even if the mining stage is avoided, tailings bioleaching could present significant risks of burden shift for mineral resource use (+322%) when applying the IMPACT WORLD + v.1.29 method but the risk disappears (-81%) with the updated CF in the v.2.01 version. While the magnitude of the impact differs in both methods, mineral resource use impacts are attributed to intensive consumption of precipitated calcium carbonate and cement for stabilization of residual tailings material. Finding a replacement for precipitated calcium carbonate will be key in mitigating climate impacts (+109–118%) and ozone depletion potential (+112%) in addition to mineral resource use risks. Land use and toxicity impacts of tailings bioleaching are not exhibiting significant risks in both IMPACT WORLD + methods in comparison to global nickel sulfate production from primary extraction (in ecoinvent). It is to note that air emissions were modelled according to the refining permit for nickel sulfide from bioheap leaching of sulfide ores<sup>51</sup>. Furthermore, a detailed accounting of emissions to water is currently missing for the conclusion to be definitive, which is a common limitation of LCIs based on pilot studies<sup>52</sup>. As a broad estimation, it can be argued that water emissions from tailings biotank leaching should not cause higher risks for burden shifts than emissions for similar hydrometallurgical circuits of bioheap leaching or POX leaching.

## Discussion

Climate change impacts reported for each processing pathway should not be taken as a single value, since the assessment of the inventory can change on a project-basis according to the localization of each step of the supply chain. Furthermore, two projects stemming from the same nickel processing pathway can exhibit differences in their flowsheets. For instance, in the process simulation for HPAL operations, electricity was assumed to be sourced from on-site sulfuric acid production, while other operations could source coal-fired electricity, a switch in electricity sourcing that can increase climate change impacts by 17 kgCO<sub>2eq</sub>/kg Ni<sub>eq</sub><sup>35</sup>. As demonstrated with the switch from coal to solar electricity for Indonesian routes, inventories developed in this work can be readily modified to account for regional differences, in addition to varying ore grade and strip ratio. While we only assess declining laterite ore grade to 0.5%, in-depth studies of the impact of declining ore grade on the resulting environmental assessment could be conducted by making use of the developed scaling method to update material and energy flows of the mining and beneficiation inventory.

It is essential to highlight that the main limitation of the scaling method is its linear scaling as a function of the mass of rock mined. In practice, the inventory is dependent on a multiplicity of factors (e.g. depth of the underground deposit, distance to drive from mine pit to comminution operations, etc.)<sup>5</sup>. Furthermore, inventories for mining and beneficiation of laterite ores are most likely exhibiting the highest uncertainty, since they were based on a disaggregation of contribution analysis data. All in all, the scaling method was developed to palliate scarce reporting of primary data for mines.

Such a lack of publicly available data on mining inventories as well as tailings management of laterite ore extraction reflects the difficulty of correctly assessing impact categories other than climate change. For example, land transformation impacts of laterite mining in Indonesia were recently reassessed as 20 times higher than previous estimates, using Google Earth imagery<sup>28</sup>. Furthermore, only project-specific data on waste composition and disposal method can reasonably depict potential environmental impacts of process waste for each site<sup>49</sup>. A complete inventory for overburden and slag disposal are not publicly available for the RKEF-NPI route. Similarly, for bioheap leaching, lack of modelling details for the overburden, precipitates and tailings forced their exclusion from the assessed inventory. However, it seems that there is a high potential for reuse of process waste within bioheap operations, with Terrafame already exhibiting a 26% reuse rate in 2023<sup>53</sup>.

For the HPAL route, only partial dry tailings compositions (adding to 66% of the dry mass) are available in the existing literature<sup>54</sup>, and do not include all toxic elements that should be found in tailings. The most comprehensive tailings composition assessment was found in a company's

sustainability report<sup>55</sup>, and only covered 62% of the dry mass. Nevertheless, toxic elements were comprehensively quantified in the report. Reported toxicity data was used to create a tailings impoundment model specific to the tailings' composition and the region's climatic conditions<sup>56</sup>. The staggering increase in carcinogenic human toxicity (+7735% change for HPAL in Fig. 4) is explained by the lack of tailings impoundment model for HPAL laterite residues in the ecoinvent database. The most contributing flow (90%) is chromium VI emission to groundwater, also acknowledged in the referenced company sustainability report<sup>55</sup>. The energy consumption during dry stacking operations (e.g. belt filter press, conveyor or trucking of tailings) as well as geotextiles usage<sup>57</sup> were excluded from the inventory due to data unavailability. Thus, while the modelled inventories provide a reliable first estimate, increased data collection is required before definitely concluding on burden shifting risks.

Also important to note, climate change impacts calculated for both pressure oxidation leaching (4.1 vs 4.4 kgCO<sub>2eq</sub>/kg nickel class I<sup>58</sup>) and bioheap leaching (7.66 vs 7.95 kgCO<sub>2eq</sub>/kg Ni<sub>eq</sub><sup>59</sup>) stand slightly under carbon footprint values disclosed publicly by both companies. This result is first likely due to the variability in reference years selected for the inventory. In this study, concentrate processing inventories were developed from environmental impact assessments containing preliminary inventories developed from steady state mass and energy balances. For POX leaching, the underestimation most probably arises from the scaling of the mining and beneficiation inventory using the ecoinvent dataset. In addition, different background datasets may have been used for impact assessment. Allocation of impacts for co-produced metals may also differ. In the present study, mass allocation was selected to avoid risks of changing results with volatile metal prices. However, economic allocation is often used by the nickel industry<sup>60</sup>, and other studies may present climate impacts of flash smelting under a combination of economic and mass allocation, to credit the co-production of cobalt, sulfuric acid and of heat recovery, yielding to a decrease of 5–8 kg CO<sub>2eq</sub>/kg Ni<sub>eq</sub><sup>35,42</sup>. Most importantly, the observed difference reinforces the need for companies to disclose actualized primary data after the preliminary environmental impact study.

Sensitivity analyses should be performed on chemical sourcing, particularly for hydrometallurgy and bioleaching pathways, since it could have a significant influence on climate change impacts, in some instances more than the energy mix. For instance, for the bioleaching of sulfidic mine tailings, switching the emission factor for electricity from the Swedish production mix (0.02 kgCO<sub>2eq</sub>/kWh) to electricity production from hard coal (1.10 kgCO<sub>2eq</sub>/kWh) negligibly impacted the overall climate change impacts from 37.6 to 37.9 kgCO<sub>2eq</sub>/kg Ni in nickel sulfide, or 0.8% change. Conducting a sensitivity analysis on the sourcing market (changing from European (RER) to a global market (RoW)) of the three main contributing chemicals to climate impacts of tailings bioleaching, in decreasing order: calcium carbonate, ammonia and sulfuric acid, results in a 2% increase (from 40.5 to 41.4 kgCO<sub>2eq</sub>/kg Ni in nickel sulfate).

However, a future body of work on process granular remodelling of chemical life cycle inventories is required before insightful sensitivity analyses of chemical sourcing can be conducted. Indeed, background data from ecoinvent is most likely severely underestimating potential climate impacts from chemicals<sup>61</sup>. Therefore, in-depth studies of chemical production methods must be undertaken in order to correctly assess the decarbonization potential of nickel processing pathways, especially for hydrometallurgy and bioleaching pathways. While harder-to-abate climate impacts from hydrometallurgy routes rely on changing or sourcing diligently chemicals used in their flowsheets, deep decarbonization of smelting routes requires a switch to bio-fuels and bio-reductants. It is important to note that if not captured, direct CO<sub>2</sub> emissions from bio-consumables will still occur at the same rate as their fossil counterparts but will be accounted for as biogenic emissions. Timeframes and scenarios specific to new production methods for chemicals and reductants used in nickel processing pathways remain to be developed in prospective background modelling tools<sup>15</sup>.

In addition, further research is required on how to cohesively model the share of primary and secondary routes in market scenarios for both current

and prospective studies. Secondary materials are expected to make up a large share of raw materials intake in the 2040 horizon<sup>62,63</sup>. In part due to the lack of harmonized scenarios for secondary material shares, recycling processing pathways were excluded from the present work primarily because the computation of environmental impacts from recycled materials is heavily dependent on the underlying methodology to allocate impacts to co-recovered metals. Beyond relieving extraction pressure on the environment, hydrometallurgical recycling could provide nickel at a carbon footprint of 7.7 kgCO<sub>2eq</sub>/kg nickel in nickel sulfate (mass allocation-based), with projected improvements to 5.4 kgCO<sub>2eq</sub>/kg Ni<sup>31</sup>. This range of carbon footprints coincides with the ones of emerging bioheap leaching (7.7 kgCO<sub>2eq</sub>/kg Ni) and established POX leaching (4.8 kgCO<sub>2eq</sub>/kg Ni) hydrometallurgical pathways assessed in our study. A recent life cycle comparison of refined metals from lithium cobalt oxide (LCO) smartphone cathode recycling versus conventional mining supply chains reports a reduction of 55%, 42% and 58% for energy consumption, CO<sub>2</sub> emissions and water consumption respectively<sup>34</sup>. Nevertheless, hydrometallurgical processing of e-waste has yet to reach a commercial scale that can provide disaggregated life cycle datasets for nickel.

The present work is an important first step towards improved granularity in current and prospective studies of mineral-intensive industrial ecosystems. Our process-based method for background modelling demonstrates variability in impacts arising from increased granularity in terms of technological representativeness. Expressly for nickel sourcing of an NMC-811 cell, climate impacts may vary by 74 kgCO<sub>2eq</sub>/kWh. Provided contribution analyses allow to readily identify key prospective improvements to climate change impacts of six nickel production pathways expected to represent the current to medium-term market. It is found that both hydrometallurgy and bioleaching impacts are mainly driven by embodied chemicals in their flowsheets. Pyrometallurgy pathways present limited opportunities for decarbonization in the short term as they will rely on new furnace configurations or the development of bio-based alternatives for fossil fuel reductants and renewable electricity infrastructure deployment.

All in all, POX leaching showcases the lowest carbon footprint (4.8 kgCO<sub>2eq</sub>/kg Ni) and no risks of burden shift, harnessing Canadian Newfoundland's hydropower. On the other hand, RKEF-NPI presents numerous risks of burden shift as well as a ~29 × higher carbon footprint (139.6 kgCO<sub>2eq</sub>/kg Ni) mainly due to Indonesia's reliance on coal for both electricity generation (61% of overall climate impacts) and pyrometallurgical reductants (31%). While Indonesia committed to decarbonize its power sector by 2060 using 60% solar<sup>64</sup>, switching from a coal-based to a fully solar-based grid for industrial activities could considerably reduce climate impacts of Indonesian nickel, by 59% for RKEF-NPI and 46% for HPAL.

Emerging bioleaching pathways are significantly less energy intensive than their pyrometallurgical sulfide processing counterparts but still exhibit comparable climate impacts due to higher material consumption from the lower nickel grade of processed ores or tailings. While ~10× more ores are treated to produce 1 kg of nickel, energy consumption is ~2.5× lower for bioheap leaching than for flash smelting and the risk for particulate matter formation dissipates. In addition to repurposing a waste resource which otherwise poses a significant risk of leakage of heavy metals to the environment, tailings bioleaching promises to reduce energy consumption by ~50× and ~5× compared to the dominant RKEF-NPI and HPAL processing routes. While climate impacts of tailings bioleaching are 3× lower than those of RKEF-NPI, they are comparable to those of the coal-powered HPAL route. High climate impacts for tailings bioleaching stem from the carbon intensive precipitation of calcium carbonate required to purify tailings, which is then allocated to nickel.

A comparison with the global ecoinvent v.3.9.1 dataset for nickel sulfate reveals a lack of technological representativeness with current processing pathways, namely RKEF-NPI and HPAL processing of laterite ores. This results in grave underestimation of climate impacts of current nickel sulfate production (a potential delta of 120 kgCO<sub>2eq</sub>/kg Ni<sub>eq</sub> for the RKEF-NPI pathway). Furthermore, while it was impossible to conclude on

potential burden shifting due to incompleteness of public data for mining and tailings management of laterite ores, as well as high variations between impact assessment methods, a preliminary assessment of all impact categories was performed. Notably, the highest potential for burden shifting is toward carcinogenic human toxicity if risks of chromium VI contamination of groundwater are not monitored closely during HPAL tailings management. This finding reinforces the need to comprehensively study such parts of the inventory as tailings management which are often neglected when building LCIs for studies assessing only carbon<sup>21</sup>.

The above conclusions demonstrate the essentiality of improved technology representativeness in current and prospective background LCIs, not only for mineral processing routes but also for background chemicals and reductants. The present case study will allow for the development of a framework for reconstructing datasets used in prospective modelling. Only then can a coherent planning of battery cell industrial ecosystems be achieved under minimal environmental impacts. We envision the application of our background modelling technique to a wider set of materials expressing high impact variance in the LIB industrial ecosystem, such as graphite<sup>22</sup>, and understudied LIB supply chains, such as iron sulfate and phosphoric acid, where emerging production routes could alleviate the surplus demand from conventional production routes, as it is the case for nickel.

## Methods

### Design of a contribution algorithm

A sorting algorithm, hereby referred to as the “contribution algorithm”, was developed to explicitly describe the contribution tree data required to characterize complex process systems found in the global ecoinvent dataset. The discussion is supported by data analysis for global nickel sulfate production. Compatibility with the OpenLCA software was selected for its open-source property. The calculation of contribution data on the foremost unit process of interest is automated via the Olca-IPC Python package<sup>65</sup>, which allows for communication between the OpenLCA server, containing the ecoinvent v.3.9.1 database, and our data processing algorithm written in a python script. The following decision tree (Fig. 5) illustrates data processing steps performed by the algorithm. The application of the contribution algorithm to the global ecoinvent nickel sulfate dataset is presented in Fig. 2 and Fig. 3, along with the associated discussion.

### Proposed method to reconstruct life cycle inventories

Key steps in the reconstruction of process-disaggregated datasets are schematized in Fig. 6. Data is compiled accordingly for each stage of the value chain enclosed within the studied material system boundaries. We consider a list of all energy sources, reagents and water volumes consumed, a list of main emissions to air and water and land transformation figures for mining. When applicable, tailings production rate, disposal method and final composition are indispensable to describe potential heavy metal leakage to groundwater. For mining and beneficiation, operations that are designed in conjunction, the inventory's ore grade and strip ratio must be known in order to be scaled for the specific metal fraction of the concentrate entering the subsequent processing stage. Concentrate processing inventories are sourced from published process-based LCIs and process simulations, and data gaps are filled with publicly available complementary sources. Final refining stages are often found in pair with concentrate processing steps or can be utilized from other sources if scalable to respect the overall mass balance.

Publicly available complementary sources notably include environmental impact assessments which usually contain most life cycle inventory elements (i.e. mass and energy balance, emissions to air and water, water consumption and land transformation). Company sustainability reports also represent important complementary sources of disclosed environmental data. To note that utilizing such sources imply that the inventory should be built consistently with data applicable to the same operation year. Mass allocation is then employed to calculate

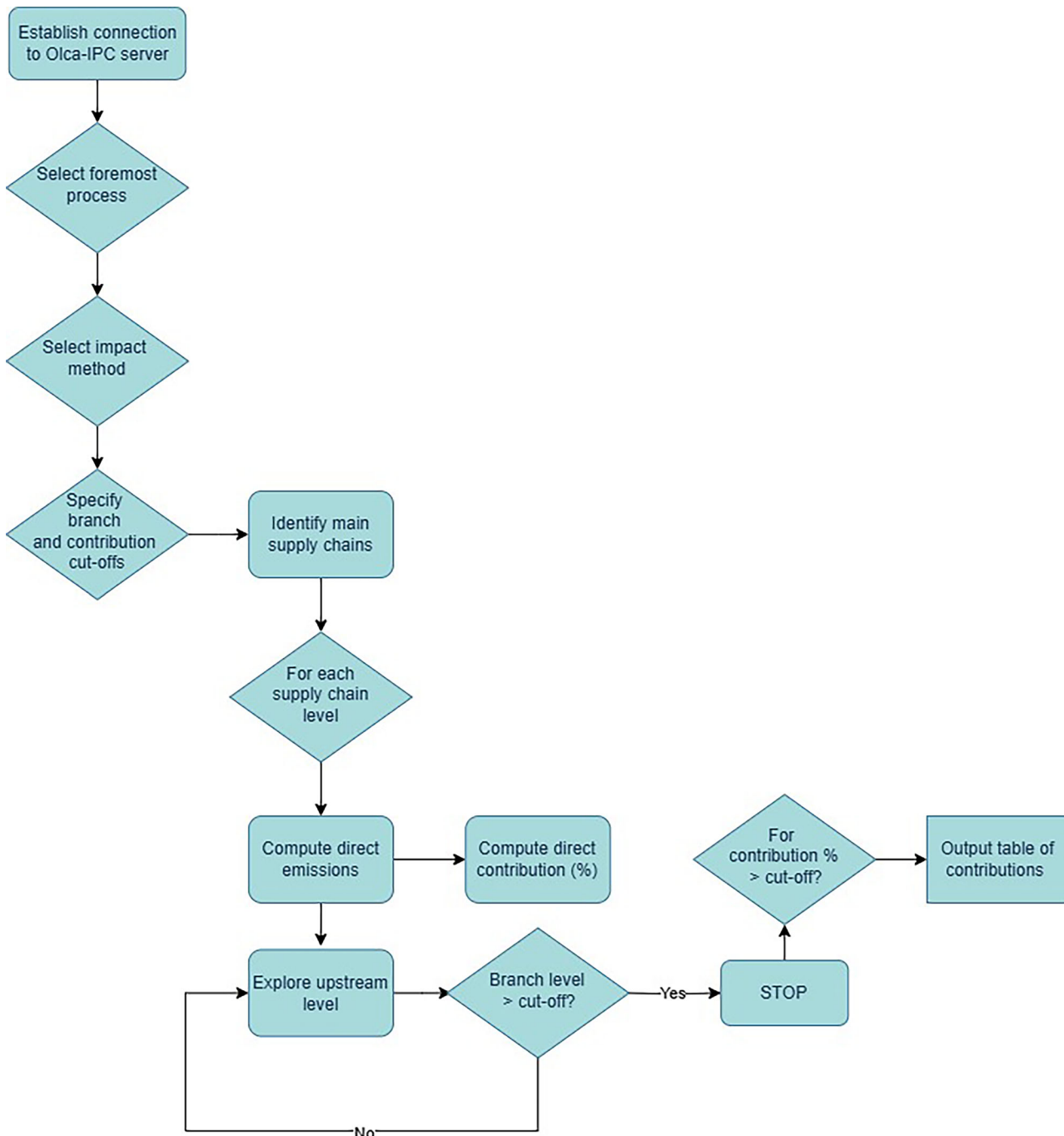


**Fig. 5 | Decision tree for the contribution algorithm.** The decision tree outlines the sequential steps undertaken to process data, from establishing server connections to calculating and summarizing impact contributions under a user-specified supply chain depth and contribution cut-off. The contribution algorithm starts by prompting the user on selecting the primary process system of interest and the

impact assessment method. Subsequently, it retrieves information on the significant supply chain branches and employs a recursive exploration method to expand upstream levels. For each expanded level, the direct emissions of contributors are computed and stored, until the limit depth is reached. Then, the algorithm outputs a table of contributions for which values are under the cut-off percentage.

impacts on a produced metal equivalent basis. Since highly probable that a portion of life cycle inventory elements are not found in reference process-based inventories, we consider it the practitioner's responsibility to find science-based models or estimates to palliate and validate data when possible, as demonstrated in the following case study on battery-grade nickel sulfate.

(through six processing routes), 4) refining to the final product. Since the state of intermediate products changes from one processing pathway to another, the functional unit is set to 1 kilogram of nickel equivalent ( $Ni_{eq}$ ) in the final product, nickel sulfate hexahydrate, battery-grade. Figure 7 depicts the considered system boundaries for inventory modelling.

### System boundaries

Reconstruction of the inventory encompasses the following steps of the value chain: 1) mining and 2) beneficiation; 3) concentrate processing

### Mining and beneficiation modelling

Primary data from the studied mine should be the prioritized source of information to compile its life cycle inventory. In the likely case of data

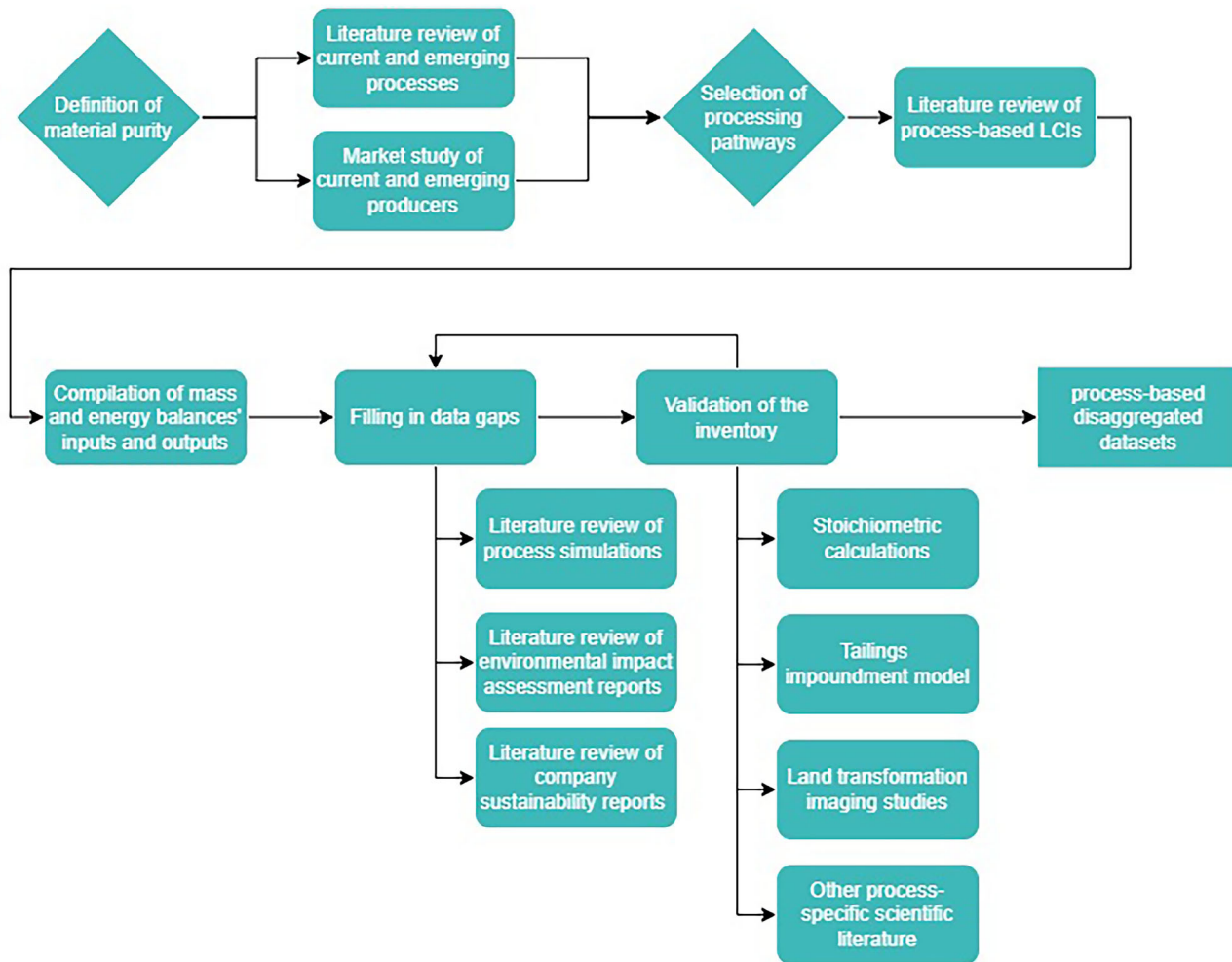


**Fig. 6 | Method for the reconstruction of process-based disaggregated inventories.** The destination of the material dictates which processing routes include the necessary refining steps to reach the required product purity. Processing routes are selected based on a combination of literature review of processing pathways as well as a market study of producers. Then, for each processing pathway, inputs and outputs are compiled from available process-based LCIs, and remaining elements

are identified as data gaps to be filled by a variety of public documentation. Compiled data from public sources is then validated via stoichiometric calculations as well as impact models and datasets from the research community, the latter being especially relevant for non-carbon impacts such as groundwater emissions from tailings and land transformation.

unavailability, we propose a methodology to adapt published inventories as a function of ore grade, strip ratio and energy mix.

The ratio of mass of waste rock displaced (namely overburden) over the mass of ore extracted is referred to as strip ratio (see Eq. 1). The strip ratio is unique to each ore deposit and varies with the type of mining operation; open-pit or underground<sup>40</sup>. It is a significative indicator of the energy and explosives consumption at a mine site, and therefore is used in pre-feasibility studies to determine the economic profitability of a deposit<sup>66</sup>.

$$\text{Strip ratio } (S) = \frac{m_{\text{overburden}}}{m_{\text{ore}}} \quad (1)$$

The total mass of rock mined is therefore defined as per Eq. 2.

$$m_{\text{rock}} = m_{\text{overburden}} + m_{\text{ore}} = (S + 1) \cdot m_{\text{ore}} \quad (2)$$

The total mass of rock mined ( $m_{\text{rock}}$ ) will be used as an approximate scaling factor ( $\lambda$ ) for the mining and beneficiation inventory. For instance, from an existing inventory of known strip ratio ( $S_1$ ); ore grade ( $x_{\text{Ni},\text{ore},1}$ ), the scaled inventory can be obtained for  $S_2$ ;  $x_{\text{Ni},\text{ore},2}$  considering that both mines share the same operation technique (open-pit or underground) and ore type (refer

to Eq. 3).

$$\lambda = \frac{m_{\text{rock},2}}{m_{\text{rock},1}} = \frac{(S_2 + 1) \cdot \frac{m_{\text{Ni},\text{concentrate},2}}{x_{\text{Ni},\text{ore},2}}}{(S_1 + 1) \cdot \frac{m_{\text{Ni},\text{concentrate},1}}{x_{\text{Ni},\text{ore},1}}} = (S_2 + 1) \cdot \frac{m_{\text{ore},2}}{m_{\text{ore},1}} \quad (3)$$

To back-calculate the specific quantity of nickel required under concentrate form ( $m_{\text{Ni},\text{concentrate}}$ ) to fulfill a final product demand ( $m_{\text{Ni},\text{final}}$ ), the nickel recovery rate ( $\eta_{\text{step}} [\%]$ ) at each step of the value chain must be considered (see Eq. 4). To note here that transport losses are neglected<sup>46</sup>.

$$m_{\text{Ni},\text{concentrate}} = \frac{m_{\text{Ni},\text{final}}}{\eta_{\text{beneficiation}} \cdot \eta_{\text{concentrate processing}} \cdot \eta_{\text{refining}}} \quad (4)$$

To obtain the total mass of concentrate required to fulfill the mass balance ( $m_{\text{concentrate}}$ ), the specific quantity of nickel required under concentrate form can simply be divided by its ore grade (Eq. 5).

$$m_{\text{concentrate}} = \frac{m_{\text{Ni},\text{concentrate}}}{x_{\text{Ni},\text{ore}}} \quad (5)$$

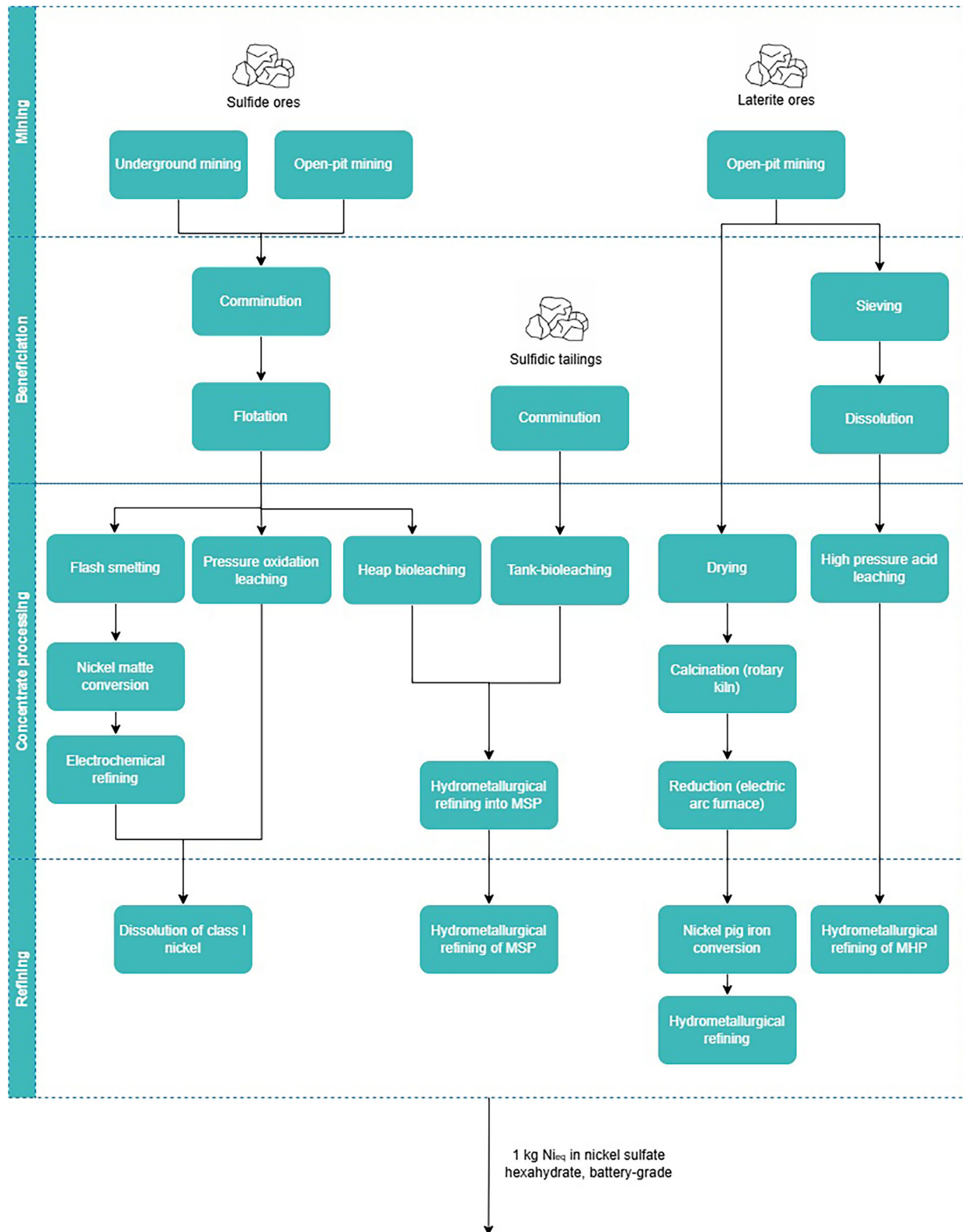


**Fig. 7 | System boundaries considered in the reconstruction of the nickel sulfate dataset.** Six nickel concentrate processing routes are expanded to encompass all steps from mining to refining to nickel sulfate hexahydrate, battery-grade. Process steps are depicted as per descriptions from the impact assessment reports or process simulations selected for life cycle inventory modelling<sup>36,42,51,67,69</sup>. Concentrate pathways are separated between treatment of sulfide ores, tailings and laterite ores. For

sulfide ores, from left to right, supply chains for flash smelting, pressure oxidation and heap bioleaching are depicted. Next, the process route for tank-bioleaching of sulfide tailings is included. For laterite ores, the supply chain for the rotary-kiln-electric-furnace pathway is represented, followed by the value chain for high pressure acid leaching.

Since the mass fraction of nickel in intermediate products may vary, the final mass of nickel assessed ( $m_{Ni,final}$ ) is set to 1 kg of  $Ni_{eq}$  for both inventories.

From there, material ( $m_i$ ) and energy ( $E_i$ ) flows can be scaled according to Eq. 6 and Eq. 7.

$$m_{i,2} = m_{i,1} \cdot \lambda [kg] \quad (6)$$

$$E_{i,2} = E_{i,1} \cdot \lambda [MJ \text{ or } kWh] \quad (7)$$

Since the inventory is scaled in units of energy, the energy source can readily be modified in the impact assessment phase. Similarly, scaling the inventory on a material flow basis allows us to consider different sourcing scenarios in the impact assessment phase.

*In terms of land use and tailings management*, since data is only available for sulfidic deposits in the ecoinvent v.3.9.1 database, estimates had to be derived for laterite deposits. To estimate land occupation and transformation impacts of laterite mining inventories, a land footprint of 0.72 m<sup>2</sup> per tonne of nickel ore extracted was applied based on imagery studies<sup>28</sup>. For tailings management, data was found for the HPAL processing route, which is recognized as the most waste intensive and presenting the highest risk of toxic contamination between laterite-processing routes<sup>49</sup>. Primary data of dry tailings composition from PT Halmahera Persada Lygend's 2022 sustainability report<sup>55</sup> was utilized to create a tailings impoundment model<sup>56</sup>. Incomplete dry tailing composition (missing 38%) was adjusted to 100% with silicon dioxide<sup>56</sup>, and the moisture content of dry stacked tailings was set to 35%<sup>55</sup>. A factor of 1.11 tonnes of tailings per tonne of laterite ore was applied to quantify the generation of tailings per tonne of nickel equivalent<sup>43</sup>.

### Process models for concentrate processing

Datasets are built by creating process models for each processing route separately, based on process data found in the literature and publicly accessible environmental impact assessments. Data collected to create process models and resulting inventories can be found in Supplementary Notes 1–6.

*For flash smelting and electrochemical refining of sulfide concentrate (16% Ni)*, the available inventory in the ecoinvent v.3.9.1 database is an aggregation of five processing routes, comprising different roasting, furnace (blast, electric or reverberatory) and refining (electro-refining, precipitation with hydrogen, electrowinning and Carbonyl process) configurations<sup>20</sup>. The corresponding inventory for mining and beneficiation of nickel concentrate (16% Ni) is based on the 2010 impact assessment study for Raglan mine operations in northern Quebec, Canada<sup>20</sup>. Even if exhibiting aggregation at the concentrate processing stage, it constitutes the most complete life cycle inventory in terms of emissions to air and water. For increased granularity at the concentrate processing stage, a published process-based inventory is used for flash smelting of sulfide ores (2.05%) and refining to nickel class I (>99.8% Ni) via ammoniacal precipitation with hydrogen<sup>42</sup>. The inventory is reassessed in a Canadian (Ontario) context. For mining and beneficiation, as well as conversion of nickel metal to nickel sulfate, we scale existing processes in the ecoinvent database.

*For pressure oxidation (POX) leaching of sulfide ores*, the nickel mine operation and beneficiation model (for nickel concentrate, 16% Ni) in ecoinvent was scaled for Voisey Bay's mine and beneficiation operations (using Eq. 3), which concentrate (19% Ni) feeds the only pressure oxidation facility currently operating in Long Harbour, Newfoundland. The inventory for hydrometallurgical processing (atmospheric chlorine leaching, pressure oxidation, impurities removal and electrowinning) was obtained from the published environmental impact assessment on Long Harbour's Commercial Nickel Processing Plant in Newfoundland, Canada<sup>67</sup>. The resulting intermediate product from Long Harbour's operations is nickel class I (>99.8% Ni), at a rate of 50,000 tonnes of nickel per annum (~47% of the Canadian battery-grade market or ~4% of the global market in 2022<sup>22</sup>).

*For bioheap leaching of low-grade sulfide ores (0.3%)*, the inventory is based on a public environmental impact assessment report from Terrafame Ltd in Finland<sup>68</sup>, which owns the only operating commercial plant

worldwide. The resulting intermediate product is mixed nickel-cobalt sulfide precipitate (43–60% Ni), including copper and zinc sulfide by-products. Mass allocation is used to tailor the dataset on a kg  $Ni_{eq}$  basis.

*For tank-bioleaching of sulfidic tailings*, a published life cycle inventory is used, which is based on a pilot plant operation of sulfidic tailings revolorization in Sweden<sup>69</sup>. The intermediate product is mixed nickel-cobalt sulfide precipitate (65% Ni), with copper and zinc sulfide by-products. Mass allocation tailors the dataset on a kg  $Ni_{eq}$  basis.

*For the rotary-kiln-electric-furnace route (RKEF)*, the laterite ore mining inventory was based on a published contribution analysis<sup>35</sup> and scaled to match the ore grade (1.22%) in the selected process simulation for RKEF processing<sup>36</sup>. The intermediate product is nickel pig iron (NPI, 2.9% Ni) which can be further processed into nickel sulfate to meet battery grade requirements. RKEF processing is assessed in the Indonesian context.

*For high pressure acid leaching (HPAL) of laterite ores*, due to unavailable environmental impact assessments at the mining stage, the laterite ore mining and beneficiation inventory is based on a published contribution analysis<sup>35</sup> and scaled to match the ore grade (1.22%) used in the selected process simulation for HPAL processing<sup>36</sup>. This HPAL inventory was supplemented with stoichiometric calculations to improve the representation of direct process CO<sub>2</sub> emissions. As such, CO<sub>2</sub> emissions arising from limestone usage in the iron and alumina removal stages were estimated based on stoichiometry of the precipitation reaction (0.44 kgCO<sub>2</sub>/kg of precipitated limestone). Sulfur burning is assumed to fulfill the HPAL process's sulfuric acid as well as electricity and high-pressure steam needs<sup>36</sup>. An existing alternative process configuration was also modelled for comparison, assuming the equivalent energy needs to be sourced from a coal-fired (lignite) power station<sup>35</sup>. Both alternatives are assessed in the Indonesian context. The resulting intermediate product is MHP at 40.87% Ni<sup>36</sup>.

### Process models for refining to nickel sulfate hexahydrate

Refining of intermediate products into nickel sulfate hexahydrate (22% Ni) is modelled as a separate process step to preserve granularity.

*The conversion of nickel class I into nickel sulfate* is based on the corresponding ecoinvent inventory. Note that the ecoinvent dataset considers the stoichiometric dissolution of nickel class I in sulfuric acid<sup>20</sup>, for a final product containing 39% Ni (anhydrous).

*For the conversion of MSP to nickel sulfate*, the inventory is based on the environmental impact assessment study for Terrafame's plan to construct a hydrometallurgical facility to convert their MSP product into nickel and cobalt sulfate meeting battery grade requirements<sup>51</sup>. The projected production rate is 170,000 tonnes of nickel sulfate hexahydrate, equivalent to 3% of the global battery-grade market in 2022<sup>22</sup>. Mass allocation is used to tailor the dataset on a kg Ni equivalent basis. The same inventory was used to complete the supply chain for MSP refining from tailings bioleaching, scaled on a kg Ni equivalent basis.

*To convert nickel pig iron exiting RKEF processing into battery-grade nickel sulfate*, the inventory is based on the same process simulation referenced for concentrate processing<sup>36</sup>. It models a circuit of pressure leaching with sulfuric acid and air, neutralization with limestone to precipitate iron and chromium impurities, nickel electrolysis to metal, re-dissolution and evaporative crystallization as nickel sulfate.

*For the conversion of MHP to nickel sulfate*, three circuits are available in the referenced study<sup>36</sup>. The first circuit for producing cobalt metal via electrolysis and nickel sulfate via double-effect evaporation was selected, as these final products better fit the battery industry's needs. MHP produced from the HPAL process is assumed to undergo this circuit to be converted into nickel sulfate.

### Impact assessment of reconstructed LCIs

For the impact assessment stage, energy steps and chemical inputs for each processing pathway were kept disaggregated by process steps following their respective flowsheets. Chemicals were assumed to be

**Table 1 | Set of assumptions for key parameters of an EV and ICEV used in equivalent distance calculations**

Parameter	Symbol	Value	Reference
Nickel content of a battery cell (kg Ni <sub>eq</sub> /kWh cell)	$m_{Ni-kWh}$	0.55	1
Rated battery capacity of an EV (kWh)	$E_{rated}$	60	72
Useable battery capacity of an EV (kWh)	$E_{useable}$	50	72
Distance driven on one EV charge (km)	$d_{charge}$	483	72
Carbon intensity of grid recharge in Quebec (kgCO <sub>2eq</sub> /kWh)	$CF_{grid}$	0.026	20
Carbon intensity of passenger car fuel combustion (kgCO <sub>2eq</sub> /L)	$CF_{gas}$	2.35	73
Average fuel consumption of an ICEV (km/L)	$F$	9.44	73
Carbon emission savings from driving an EV compared to an ICEV (kgCO <sub>2eq</sub> /km)	$\Delta_{CO_2}$	0.2	Eq. 11

sourced from continent-wide or global markets for the first assessment of developed LCIs. If a chemical is known to be produced in a specific region, the production process is used instead of the market. Electricity and heat providers were adjusted based on the current regional specificity of modelled concentrate processing pathways, where the full supply chain is assumed to take place. For climate impacts assessment, the IPCC 2013 – GWP 100 years impact method was selected, even if not most up to date, to ease results comparison with previously published studies. The IMPACT WORLD+ method (version midpoint 1.29) was selected to assess 16 other impact categories<sup>70</sup>, and was compared with its version 2.01, as well as with the ReCiPe 2016 method for midpoints with a hierarchist perspective<sup>71</sup>.

Resulting embodied carbon dioxide emissions ( $CF_{Ni}$ ) as well as embodied energy ( $E_{Ni}$ ) of each nickel processing pathway were further converted into an equivalent driving distance ( $d_{eq}$ ), according to Eq. 8 and Eq. 9 respectively. This conversion was performed to assess the impact of nickel sourcing on the life-cycle performance of an electric vehicle (EV) compared to an internal combustion engine vehicle (ICEV).

$$d_{eq, CO_2} = \frac{CF_{Ni} \cdot m_{Ni-kWh} \cdot E_{rated}}{\Delta_{CO_2}} \quad (8)$$

$$d_{eq,energy} = \frac{E_{Ni} \cdot m_{Ni-kWh} \cdot d_{charge}}{\varphi} \quad (9)$$

For the embodied energy conversion, the energetic performance of the battery pack is included as the ratio ( $\varphi$ ) of useable over rated battery capacity.

$$\varphi = \frac{E_{useable}}{E_{rated}} \quad (10)$$

The set of assumptions for the conversion to  $d_{eq}$  is presented in Table 1. Carbon emission savings from driving an EV compared to an ICEV are calculated using Eq. 11.

$$\Delta_{CO_2} = \frac{CF_{gas}}{F} - \frac{CF_{grid} \cdot E_{useable}}{d_{charge}} \quad (11)$$

## Data availability

Data is provided within the manuscript and supplementary information file S1.

## Code availability

The underlying code for this study is not publicly available but may be made available on reasonable request from the corresponding author.

## Abbreviations

CF	characterization factor
CF <sub>gas</sub>	carbon intensity of passenger car fuel combustion
CF <sub>grid</sub>	carbon intensity of grid recharge
CF <sub>Ni</sub>	embodied carbon dioxide emissions of nickel
CTU	comparative toxic units
d <sub>charge</sub>	distance driven on one EV charge
d <sub>eq</sub>	equivalent driving distance
E <sub>i</sub>	energy flow
E <sub>Ni</sub>	embodied energy of nickel
E <sub>rated</sub>	rated battery capacity of an EV
E <sub>useable</sub>	useable battery capacity of an EV
EPAL	enhanced pressure acid leaching
EV	electric vehicle
F	average fuel consumption of an ICEV
FAP	freshwater acidification (kgSO <sub>2eq</sub> )
FEP	freshwater eutrophication (kgPO <sub>4</sub> , P-lim <sub>eq</sub> )
FETP	freshwater ecotoxicity (CTUh)
FNEU	fossil and nuclear energy use (MJ deprived)
GLO	global
GWP-1	climate change, long term (kgCO <sub>2eq</sub> )
GWP-s	climate change, short term (kgCO <sub>2eq</sub> )
HPAL	high-pressure acid leaching
HTP-c	human toxicity cancer (CTUh)
HTP-nc	human toxicity non cancer (CTUh)
IAMs	integrated assessment models
ICEV	internal combustion engine vehicle
IR	ionizing radiations (Bq C-14 <sub>eq</sub> )
LCA	life cycle assessment
LCIs	life cycle inventories
LCO	lithium cobalt oxide
LFP	lithium iron phosphate
LIB	lithium-ion battery
LU-o	land occupation, biodiversity (m <sup>2</sup> arable land <sub>eq</sub> · yr)
LU-t	land transformation, biodiversity (m <sup>2</sup> arable land <sub>eq</sub> )
m <sub>concentrate</sub>	mass of concentrate
MEP	marine eutrophication (kg N, N-lim <sub>eq</sub> )
MHP	mixed hydroxide precipitate
m <sub>i</sub>	material flow
m <sub>Ni,concentrate</sub>	mass of nickel under concentrate form
m <sub>Ni,final</sub>	mass of nickel in the final product
m <sub>Ni-kWh</sub>	nickel content of a battery cell
m <sub>ore</sub>	mass of ore
m <sub>overburden</sub>	mass of overburden
m <sub>rock</sub>	mass of rock
MRU	mineral resources use (kg deprived)
MSP	mixed sulfide precipitate
Ni <sub>eq</sub>	nickel equivalent
NMC-811	nickel-manganese-cobalt in 80%, 10%, 10% molar proportion.
NMVOC	non-methane volatile compounds
NPI	nickel pig iron
ODP	ozone layer depletion (kg CFC-11 <sub>eq</sub> )
PLCA	prospective life cycle assessment
PMF	particulate matter formation (kg PM2.5 <sub>eq</sub> )
POF	photochemical oxidant formation (kg NMVOC <sub>eq</sub> )
POX	pressure oxidation leaching
RER	European region
RoW	rest-of-world, global market
RKEF	rotary kiln electric furnace
S	strip ratio
TAP	terrestrial acidification (kg SO <sub>2eq</sub> )
WU	water scarcity (m <sup>3</sup> world <sub>eq</sub> )
x <sub>Ni,ore</sub>	mass fraction of nickel in the ore

$\Delta CO_2$	carbon emission savings from driving an EV compared to an ICEV
$\eta_{step}$	mass recovery rate for a processing step
$\lambda$	scaling factor for the mining and beneficiation inventory
$\varphi$	ratio of useable over rated battery capacity

Received: 13 December 2024; Accepted: 27 April 2025;

Published online: 03 June 2025

## References

- Chordia, M., Nordelöf, A. & Ellingsen, L. A.-W. Environmental life cycle implications of upscaling lithium-ion battery production. *The International Journal of Life Cycle Assessment* **26**, 2024–2039 (2021).
- Erakca, M. et al. Closing gaps in LCA of lithium-ion batteries: LCA of lab-scale cell production with new primary data. *Journal of Cleaner Production* **384**, 135510 (2023).
- Manjong, N. B., Usai, L., Orangi, S., Clos, D. P. & Strømman, A. H. Exploring raw material contributions to the greenhouse gas emissions of lithium-ion battery production. *Journal of Energy Storage* **100**, 113566 (2024).
- Ali, A.-R., Lackner, J., Cerdas, F. & Herrmann, C. Analysis of nickel sulphate datasets used in lithium-ion batteries. *Procedia CIRP* **116**, 348–353 (2023).
- Manjong, N. B., Usai, L., Burheim, O. S. & Strømman, A. H. Life Cycle Modelling of Extraction and Processing of Battery Minerals—A Parametric Approach. *Batteries* **7**, 57 (2021).
- Weidner, T., Tulus, V. & Guillén-Gosálbez, G. Environmental sustainability assessment of large-scale hydrogen production using prospective life cycle analysis. *International Journal of Hydrogen Energy* **48**, 8310–8327 (2023).
- Xu, C. et al. Future greenhouse gas emissions of automotive lithium-ion battery cell production. *Resources, Conservation and Recycling* **187**, 106606 (2022).
- Hung, C. R., Kishimoto, P., Krey, V., Strømman, A. H. & Majeau-Bettez, G. ECOPT2: An adaptable life cycle assessment model for the environmentally constrained optimization of prospective technology transitions. *Journal of Industrial Ecology* **26**, 1616–1630 (2022).
- van der Meide, M., Harpprecht, C., Northey, S., Yang, Y. & Steubing, B. Effects of the energy transition on environmental impacts of cobalt supply: A prospective life cycle assessment study on future supply of cobalt. *Journal of Industrial Ecology* **26**, 1631–1645 (2022).
- Harpprecht, C., van Oers, L., Northey, S. A., Yang, Y. & Steubing, B. Environmental impacts of key metals' supply and low-carbon technologies are likely to decrease in the future. *Journal of Industrial Ecology* **25**, 1543–1559 (2021).
- Charalambous, M. A., Sacchi, R., Tulus, V. & Guillén-Gosálbez, G. Integrating emerging technologies deployed at scale within prospective life cycle assessments. *Sustainable Production and Consumption*, <https://doi.org/10.1016/j.spc.2024.08.016> (2024).
- Sacchi, R. & Hahn-Menacho, A. J. pathways: life cycle assessment of energy transition scenarios. *Journal of Open Source Software* **9**, 7309 (2024).
- Kuipers, K. J. J., van Oers, L. F. C. M., Verboon, M. & van der Voet, E. Assessing environmental implications associated with global copper demand and supply scenarios from 2010 to 2050. *Global Environmental Change* **49**, 106–115 (2018).
- Van der Voet, E., Van Oers, L., Verboon, M. & Kuipers, K. Environmental Implications of Future Demand Scenarios for Metals: Methodology and Application to the Case of Seven Major Metals. *Journal of Industrial Ecology* **23**, 141–155 (2019).
- Sacchi, R. et al. PRospective EnvironMental Impact asSEment (premise): A streamlined approach to producing databases for prospective life cycle assessment using integrated assessment models. *Renewable and Sustainable Energy Reviews* **160**, 112311 (2022).
- Crenna, E., Gauch, M., Widmer, R., Wäger, P. & Hischier, R. Towards more flexibility and transparency in life cycle inventories for Lithium-ion batteries. *Resources, Conservation and Recycling* **170**, 105619 (2021).
- Schmidt, T. S. et al. Additional Emissions and Cost from Storing Electricity in Stationary Battery Systems. *Environmental Science & Technology* **53**, 3379–3390 (2019).
- von Drachenfels, N., Husmann, J., Khalid, U., Cerdas, F. & Herrmann, C. Life Cycle Assessment of the Battery Cell Production: Using a Modular Material and Energy Flow Model to Assess Product and Process Innovations. *Energy Technology* **11**, 2200673 (2023).
- Šimaitis, J., Allen, S. & Vagg, C. Are future recycling benefits misleading? Prospective life cycle assessment of lithium-ion batteries. *Journal of Industrial Ecology* **n/a**, <https://doi.org/10.1111/jiec.13413> (2023).
- Wernet, G. et al. The ecoinvent database version 3 (part I): overview and methodology. *The International Journal of Life Cycle Assessment* **21**, 1218–1230 (2016).
- Istrate, R. et al. Decarbonizing lithium-ion battery primary raw materials supply chain. *Joule* **8**, 2992–3016 (2024).
- Peiseler, L. et al. Carbon Footprint Distributions of Lithium-Ion Batteries and Their Materials. *Nature Communications* **15**, 10301 (2024).
- IEA. Nickel, <https://www.iea.org/reports/nickel> (2024).
- Winjobi, O., Kelly, J. C. & Dai, Q. Life-cycle analysis, by global region, of automotive lithium-ion nickel manganese cobalt batteries of varying nickel content. *Sustainable Materials and Technologies* **32**, e00415 (2022).
- Harpprecht, C. et al. Future environmental impacts of metals: A systematic review of impact trends, modelling approaches, and challenges. *Resources, Conservation and Recycling* **205**, 107572 (2024).
- Nickel-Institute. Life cycle data - Executive Summary, <https://nickelinstitute.org/media/fbmdel4y/lifecycledata-summary-updatejan2023.pdf> (2023).
- Milewski, A. Mixed hydroxide precipitate — the new class one nickel, <https://www.mining.com/mixed-hydroxide-precipitate-the-new-class-one-nickel/> (2021).
- Heijlen, W. & Duhayon, C. An empirical estimate of the land footprint of nickel from laterite mining in Indonesia. *The Extractive Industries and Society* **17**, 101421 (2024).
- Khoo, J. Z., Haque, N., Woodbridge, G., McDonald, R. & Bhattacharya, S. A life cycle assessment of a new laterite processing technology. *Journal of Cleaner Production* **142**, 1765–1777 (2017).
- Johnson, D. B., Bryan, C. G., Schlömann, M. & Roberto, F. F. *Biomining Technologies*. (Springer, 2023).
- Ali, A.-R. et al. Simulation-based life cycle assessment of secondary materials from recycling of lithium-ion batteries. *Resources, Conservation and Recycling* **202**, 107384 (2024).
- Hanna, F., Yuan, L., Somers, C. & Anctil, A. Spatio-Temporal Life Cycle Assessment of NMC111 Hydrometallurgical Recycling in the US. *Technology Innovation for the Circular Economy: Recycling, Remanufacturing, Design, Systems Analysis and Logistics*, 297–308 (2024).
- Roberto, F. F. & Schippers, A. Progress in bioleaching: part B, applications of microbial processes by the minerals industries. *Applied Microbiology and Biotechnology* **106**, 5913–5928 (2022).
- Machala, M. L. et al. Life cycle comparison of industrial-scale lithium-ion battery recycling and mining supply chains. *Nature Communications* **16**, 988, <https://doi.org/10.1038/s41467-025-56063-x> (2025).
- Tijsseling, L. & Whattoff, P. Product carbon footprint of nickel sulfate hexahydrate production. (2023).
- Dry, M., Vaughan, J. & Hawker, W. Environmental evaluation of making nickel sulphate. (2019).
- Pandey, N., Tripathy, S. K., Patra, S. K. & Jha, G. Recent Progress in Hydrometallurgical Processing of Nickel Lateritic Ore. *Transactions of the Indian Institute of Metals* **76**, 11–30 (2023).

38. Norgate, T. & Jahanshahi, S. Assessing the energy and greenhouse gas footprints of nickel laterite processing. *Minerals Engineering* **24**, 698–707 (2011).
39. Iyer, R. K. & Kelly, J. C. Life-Cycle Inventory of Critical Materials: Nickel, Copper, Titanium, and Rare-Earth Elements. (Argonne National Laboratory (ANL), Argonne, IL (United States), 2022).
40. Schneider, E., Carlsen, B., Tavrides, E., van der Hoeven, C. & Phathanapirom, U. A top-down assessment of energy, water and land use in uranium mining, milling, and refining. *Energy Economics* **40**, 911–926 (2013).
41. Gerber, L., Fazlollahi, S. & Maréchal, F. A systematic methodology for the environmental design and synthesis of energy systems combining process integration, Life Cycle Assessment and industrial ecology. *Computers & Chemical Engineering* **59**, 2–16 (2013).
42. Wei, W., Samuelsson, P. B., Tillander, A., Gyllenram, R. & Jönsson, P. G. Energy Consumption and Greenhouse Gas Emissions of Nickel Products. *Energies* **13**, 5664 (2020).
43. Bartzas, G. & Komnitsas, K. Cradle to gate life-cycle assessment of battery grade nickel sulphate production through high-pressure acid leaching. *Science of The Total Environment* **952**, 175902 (2024).
44. Abdelbaky, M. et al. Global warming potential of lithium-ion battery cell production: Determining influential primary and secondary raw material supply routes. *Cleaner Logistics and Supply Chain* **9**, 100130 (2023).
45. Norgate, T. & Jahanshahi, S. Energy and greenhouse gas implications of deteriorating quality ore reserves. *5th Australian conference on life cycle assessment: achieving business benefits from managing life cycle impacts* (2006).
46. Eckelman, M. J. Facility-level energy and greenhouse gas life-cycle assessment of the global nickel industry. *Resources, Conservation and Recycling* **54**, 256–266 (2010).
47. Mercier, G., Pasquier, L.-C., Kemache, N., Cecchi, E. & Blais, J.-F. Production of Low Carbon Footprint Magnesia. WO/2018/018137 (2017).
48. Cox, B., Bauer, C., Mendoza Beltran, A., van Vuuren, D. P. & Mutel, C. L. Life cycle environmental and cost comparison of current and future passenger cars under different energy scenarios. *Applied Energy* **269**, 115021 (2020).
49. Bartzas, G., Tsakiridis, P. E. & Komnitsas, K. Nickel industry: Heavy metal(loid)s contamination - sources, environmental impacts and recent advances on waste valorization. *Current Opinion in Environmental Science & Health* **21**, 100253 (2021).
50. IMPACTWORLD+. *IMPACT World+ Version 2.0*, <https://www.impactworldplus.org/version-2-0/> (2024).
51. Terrafame. *Permit PSAVI/3626/2019: Environmental permit of the battery chemical factory, Sotkamo (translated from finnish) Akkukemikaalitehtaan ympäristöluupa, Sotkamo*, <https://ylupa.avi.fi/fi-FI> (2021).
52. Tsoy, N., Steubing, B., van der Giesen, C. & Guinée, J. Upscaling methods used in ex ante life cycle assessment of emerging technologies: a review. *The International Journal of Life Cycle Assessment* **25**, 1680–1692, <https://doi.org/10.1007/s11367-020-01796-8> (2020).
53. Terrafame. *Strengthening a transparent battery value chain - sustainability review 2024*, [https://www.terrafame.com/media/mediamateriaali/raportointi/kestavan-kehityksen-katsaukset/eng/terrafame\\_katsaus\\_2024\\_en.pdf](https://www.terrafame.com/media/mediamateriaali/raportointi/kestavan-kehityksen-katsaukset/eng/terrafame_katsaus_2024_en.pdf) (2024).
54. Wu, J., Ma, B., Chen, Y., Yang, H. & Wang, C. Sulfur Removal and Iron Recovery from High-Pressure Acid Leaching Residue of Nickel Laterite Ore. *Journal of Sustainable Metallurgy*, <https://doi.org/10.1007/s40831-024-00853-y> (2024).
55. Lygend. 2022 Sustainability Update Report, <https://hpnickel.com/files/download/sustainability/PTHPAL-SUR-2022-compressed.pdf> (2022).
56. Doka, G. *A model for waste-specific and climate-specific life cycle inventories of tailings impoundments – Version 2*, <http://www.doka.ch/publications.htm> (2018).
57. Adrianto, L. R., Ciacci, L., Pfister, S. & Hellweg, S. Toward sustainable reprocessing and valorization of sulfidic copper tailings: Scenarios and prospective LCA. *Science of The Total Environment* **871**, 162038 (2023).
58. Vale. *Low-carbon nickel positions Vale well in North American, European electric vehicle market* <https://www.vale.com/documents/d/guest/low-carbon-vale> (2020).
59. Terrafame. *Terrafame's nickel sulphate production offers the lowest carbon footprint in the industry - altogether 60% lower than in existing conventional processes*, <https://www.terrafame.com/newsroom/media-releases/terrafames-nickel-sulphate-production-offers-the-lowest-carbon-footprint-in-the-industry-altogether-60-lower-than-in-existing-conventional-processes.html?p461=7> (2020).
60. Mistry, M., Gediga, J. & Boonzaier, S. Life cycle assessment of nickel products. *The International Journal of Life Cycle Assessment* **21**, 1559–1572 (2016).
61. Oberschelp C., et al Poor data and outdated methods sabotage the decarbonization efforts of the chemical industry. *ChemRxiv*, <https://doi.org/10.26434/chemrxiv-2023-8c86t> (2023).
62. Kumar, A., Huyn, P. & Vennelakanti, R. A digital solution framework for enabling electric vehicle battery circularity based on an ecosystem value optimization approach. *npj Materials Sustainability* **1**, <https://doi.org/10.1038/s44296-023-00001-9> (2023).
63. Economist. *Most electric-car batteries could soon be made by recycling old ones*, <https://www.economist.com/science-and-technology/2024/09/19/most-electric-car-batteries-could-soon-be-made-by-recycling-old-ones> (2024).
64. Kawai, K. Y., Kyohei. *Indonesia Using Nuclear Power to Decarbonize and How Japan Can Contribute*, <https://www.mri.co.jp/en/knowledge/insight/20240214.html> (2024).
65. Srocka, M. Olca-IPC. In GitHub repository., <https://github.com/GreenDelta/olca-ipc.py> (2023).
66. Darling, P., Society for Mining, M. & Exploration. *SME Mining Engineering Handbook, Third Edition*. (Society for Mining, Metallurgy, and Exploration, 2011).
67. Vale. *Environmental Impact Statement Long Harbour Commercial Nickel Processing Plant*, <https://www.gov.nl.ca/ecc/projects/project-1243/> (2008).
68. Terrafame. *Permit PSAVI/2461/2017: Terrafame Oy's Sotkamo mining and metal production environmental and water management permit, as well as the soil and environmental permit for the extraction, extraction and crushing of rock material (translated from finnish)* Terrafame Oy:n Sotkamon kaivos- ja metallituotannon ympäristö- ja vesitalouslupa sekä kalliolikviajaineksen ottoa, louhinta ja murskausta koskeva maa-aines- ja ympäristölupa, <https://ylupa.avi.fi/fi-FI> (2022).
69. Di Maria, A., Khoshkhoo, M., Sand, A. & Van Acker, K. Towards sustainable resource valorization: A life cycle sustainability assessment of metals recovery from sulfidic mining residues in Sweden. *Resources, Conservation and Recycling* **204**, 107513 (2024).
70. Bulle, C. et al. IMPACT World+: a globally regionalized life cycle impact assessment method. *The International Journal of Life Cycle Assessment* **24**, 1653–1674 (2019).
71. Huijbregts, M. A. J. et al. ReCiPe2016: a harmonised life cycle impact assessment method at midpoint and endpoint level. *The International Journal of Life Cycle Assessment* **22**, 138–147 (2017).
72. ANL. *Technoeconomic Analysis of Chemical and Electrochemical Technologies*, <https://www.anl.gov/cse/electrochemical-chemical-TEA> (2024).

73. EPA. *Greenhouse Gas Emissions from a Typical Passenger Vehicle*, <https://www.epa.gov/greenvehicles/greenhouse-gas-emissions-typical-passenger-vehicle> (2024).

## Acknowledgements

The authors would like to thank Anna Lyrvall and Lovisa Wennberg for the insightful conversations on the sustainability of battery-grade nickel supply chains during conceptualization and analysis. Funding by the Natural Sciences and Engineering Research Council of Canada is gratefully acknowledged.

## Author contributions

S.R. performed the underlying conceptualization and data analysis, as well as writing of the manuscript. H.M. designed the contribution algorithm used for the analysis of the nickel sulfate dataset. K.V., J-P.H. and L.F. provided insightful feedback throughout conceptualization, data analysis and revision of the manuscript.

## Competing interests

The authors declare no competing interests.

## Additional information

**Supplementary information** The online version contains supplementary material available at <https://doi.org/10.1038/s44296-025-00059-7>.

**Correspondence** and requests for materials should be addressed to Louis Fradette.

**Reprints and permissions information** is available at <http://www.nature.com/reprints>

**Publisher's note** Springer Nature remains neutral with regard to jurisdictional claims in published maps and institutional affiliations.

**Open Access** This article is licensed under a Creative Commons Attribution-NonCommercial-NoDerivatives 4.0 International License, which permits any non-commercial use, sharing, distribution and reproduction in any medium or format, as long as you give appropriate credit to the original author(s) and the source, provide a link to the Creative Commons licence, and indicate if you modified the licensed material. You do not have permission under this licence to share adapted material derived from this article or parts of it. The images or other third party material in this article are included in the article's Creative Commons licence, unless indicated otherwise in a credit line to the material. If material is not included in the article's Creative Commons licence and your intended use is not permitted by statutory regulation or exceeds the permitted use, you will need to obtain permission directly from the copyright holder. To view a copy of this licence, visit <http://creativecommons.org/licenses/by-nc-nd/4.0/>.

© The Author(s) 2025, corrected publication 2025